

# Absorption of $\pi^-$ mesons by nuclei

V. S. Buttsev

*Joint Institute for Nuclear Research, Dubna*

A. S. Il'inov

*Institute of Nuclear Research, USSR Academy of Sciences, Moscow*

S. E. Chigrinov

*Institute of Heat and Mass Transfer, Belorussian Academy of Sciences, Minsk*  
Fiz. Elem. Chastits At. Yadra 11, 900-966 (July-August 1980)

Investigations into the absorption of slow  $\pi^-$  mesons by medium and heavy nuclei are reviewed. The latest experimental data in the study of a new physical phenomenon are reported: the excitation of high-spin nuclear states as a result of absorption of  $\pi^-$  mesons. The single-nucleon mechanism of absorption of  $\pi^-$  mesons is considered in connection with the problem of the existence in nuclei of a  $\pi$  condensate and  $\Delta^{++}$  baryon resonances. A method is explained for determining the relative probability of nuclear absorption of pions in chemical compounds from the induced radioactivity of the residual nucleus. The possibilities of applying this method in mesic chemistry are considered. The experimental data are analyzed in the framework of modern models of the process of absorption of  $\pi^-$  mesons by nuclei.

PACS numbers: 25.80. + f

## INTRODUCTION

The process of absorption of slow negative pions by nuclei occupies an independent position in modern physics because this phenomenon embraces different problems of mesoatomic physics, mesonuclear interaction, nuclear reactions, and nuclear structure. Investigation of this process began about three decades ago. So far, a large amount of experimental information has been accumulated, and many theoretical studies have been made, which have made it possible to understand the basic features of nuclear absorption of pions. Some of the results of these studies are reflected in the monographs and reviews of Refs. 1-10. However, the overwhelming majority of these are devoted to the case of absorption of pions by the lightest nuclei, while the more complicated but no less interesting reactions involving medium and heavy nuclei have been undeservedly neglected. The present review aims to fill this gap.

According to modern ideas, the  $\pi^-$  meson is absorbed in several stages. The negative pion stopped in matter is captured by the Coulomb field of the nucleus, as a result of which a pionic atom is formed. Its initial orbit has principal quantum number  $n \geq 20$  (Ref. 2). Then, by the emission of Auger electrons and x rays, the pion goes over to orbits with lower  $n$ , and is then absorbed by the nucleus from one of these orbits. In the case of light elements, the absorption of the pion by the nucleus occurs from the 1s orbit. The heavier the element, the closer to the nucleus are the mesoatomic orbits and the earlier is the strong interaction which leads to absorption of the pion by the nucleus effective. For example, in heavy mesic atoms the absorption of the pion takes place mainly from the 4f orbit.<sup>3</sup>

The lifetime of the  $\pi^-$  meson significantly exceeds the time of formation of the mesic atom and its de-excitation, so that effectively every pion stopped in matter is absorbed by a nucleus. In the process, the nucleus may acquire an energy equivalent to the rest mass  $m_\pi$ ,

$\approx 140$  MeV of the  $\pi^-$ . Thus, a strongly excited nucleus is obtained. Measurement of the spectra of the emitted neutrons and charged particles resulting from the de-excitation of such a nucleus, and also of the spectra of the gamma rays of the residual nuclei is of interest in at least two respects: first, to elucidate the mechanism of the actual absorption reaction and, second, to investigate the decay of highly excited nuclear matter.

Conservation of energy and momentum prevents a free nucleon from absorbing a pion, and therefore this process must be strongly suppressed in the case of an intranuclear nucleon as well.<sup>2</sup> Indeed, numerous experiments<sup>11-25</sup> have shown that several nucleons participate in the absorption of a pion by a nucleus. The first model proposed to describe the absorption of pions by nuclei was a model that considered the mechanism of two-nucleon absorption.<sup>26</sup> This model is analogous to the model of quasideuteron absorption of gamma rays.<sup>27</sup> Later, the mechanism of  $\alpha$ -particle absorption of pions was proposed.<sup>28,29</sup> Estimates were also made of the absorption of a pion by a nucleon bound in a nucleus.<sup>30,31</sup>

Investigations into the mechanism of absorption of slow  $\pi^-$  mesons are intimately related to the problem of clustering in nuclei. The question of the existence of two-nucleon clusters arose after experiments of the group of M. G. Meshcheryakov, which revealed that deuterons are knocked out of the nucleus by high-energy protons.<sup>32</sup> Later, Wilkinson put forward the idea that on the surface of a nucleus there are correlated pairs of nucleons and  $\alpha$  particles.<sup>33</sup> However, after many years of investigation there is still no answer to the question of clustering in the nucleus, nor to the question of the part played by the different mechanisms of pion absorption by nuclei. This was one of the reasons why in recent time there has been greater interest in the process of pion-nucleus absorption.

The commissioning of a new generation of accelerators giving high-intensity  $\pi^-$  beams has made it possible

to obtain new confirmations of the mechanism of many-nucleon absorption of pions. In experiments involving heavy nuclei, initially at Dubna<sup>34,35</sup> and later at SIN<sup>36,37</sup> and CERN,<sup>38</sup> there was discovered the previously unknown phenomenon of excitation of high-spin (up to 12–19 $\hbar$ ) states of the residual nucleus. Until recently, the origin of the large angular momentum of the residual nucleus remained unclear, since the angular momentum introduced by the pion does not exceed 3 $\hbar$ . The explanation of the phenomenon of excitation of high-spin states was also found on the basis of the notion of many-nucleon absorption of pions.<sup>40</sup>

No less important is another aspect associated with the investigation of the properties of the highly excited nuclei formed after pion absorption. Since the excitation energy  $E^*$  of the nucleus can reach a large value  $\sim m_\pi$ , the process may be accompanied by strong disintegration of the nucleus. Indeed, experiments showed<sup>22,35</sup> that with large probability up to 17 nucleons can be carried away from a heavy target nucleus and that nuclei with large neutron deficit are observed among the produced isotopes.

In addition, pion absorption reactions result in fission of medium nuclei with atomic number  $A \leq 150$  (Ref. 41). Earlier, processes of strong disintegration and fission of medium nuclei were observed only in reactions involving high-energy particles.

Thus, the process of absorption of slow  $\pi^-$  mesons by nuclei combines features of low-energy and high-energy nuclear reactions. To describe this process, models have been developed (Refs. 39, 40, 42, and 44) that explain the observed effects and establish a connection between the mechanism of absorption of slow  $\pi^-$  mesons and nuclear reactions initiated by high-energy particles. Let us now consider these models.

## 1. GENERAL PICTURE OF THE PROCESS AND METHODS OF DESCRIBING IT

The most popular contemporary models<sup>40,42,44</sup> regard the process of pion absorption as a multistage process.

**Formation and De-Excitation of the Pionic Atom.** As we have already noted, in the initial stage the negative pion stopped in matter is captured by the Coulomb field of a nucleus, as a result of which a highly excited mesic atom is formed. The process of de-excitation of the atom, which consists of transitions of the pion to lower orbits accompanied by the emission of Auger electrons and x rays, ceases with the absorption of the pion from one of the mesoatomic orbits. Obviously, the pion will be absorbed from the orbits for which its wave function overlaps with the nucleus.

To understand the process as a whole, it is necessary to know the radial dependence of the probability of absorption  $P_{\text{abs}}(r)$  by the nucleus. For the probability of absorption of a pion from a state with given values of the principal and orbital quantum numbers  $n$  and  $l$  we have

$$P_{nl}(r) \sim r^2 \rho(r) |\psi_{nl}(r)|^2, \quad (1)$$

where  $\rho(r)$  is the density of the nuclear matter, and

$\psi_{nl}(r)$  is the pion wave function. The expression (1) must then be summed over all states of the mesic atom in accordance with their population, which is determined by the level widths  $\Gamma_{nl}$  and the initial distribution over  $n$  and  $l$  of the pions captured by the Coulomb field of the nucleus.

One can obtain the form of the function  $P_{\text{abs}}(r)$  without calculating the level population of the pionic atom by analyzing only experimental data on x-ray transitions in pionic atoms<sup>3</sup> and the calculated<sup>43</sup> wave functions  $\psi_{nl}(r)$ . On the basis of such an analysis, the authors of Ref. 40 suggested that in medium and heavy nuclei the pion is absorbed in the surface layer of the nucleus. As a first approximation, the pion absorption probability density in the nucleus was taken in the form

$$P_{\text{abs}}(r) \sim \exp \{ -[r - (C + \Delta r)]^2 / 2\sigma^2 \}, \quad (2)$$

where  $\sigma = 1.3 \times 10^{-13}$  cm, and  $C$  is a parameter in the nuclear matter density distribution:

$$\rho(r) = \rho_0 \{ 1 + \exp[(r - C)/a] \}^{-1}. \quad (3)$$

The values of the parameters in the expression (3) are taken from experiments on the scattering of electrons by nuclei:  $a = 0.545 \times 10^{-13}$  cm and  $C = 1.07A^{1/3} 10^{-13}$  cm. The parameter  $\Delta r \geq 0$  characterizes the shift of the maximum of the Gaussian curve that describes  $P_{\text{abs}}(r)$  relative to the radius at which the density has fallen to the half-value. In Ref. 40,  $\Delta r$  was determined from the condition of best matching to the experimental data on the absorption of  $\pi^-$  mesons by nuclei.

Recently, Orth *et al.*<sup>44</sup> made a systematic calculation of the pion absorption probability, beginning with the formation of the pionic atom and ending with its de-excitation. The calculation of the pionic atom was based on the method developed in Refs. 45 and 46. This confirmed the correctness of the assumption made earlier in Ref. 40 concerning the surface nature of pion absorption by nuclei. As can be seen in Fig. 1,  $\Delta r = 0$ , and the parameter describing the width of the Gaussian curve has a value smaller than in Ref. 40:  $\sigma \approx 0.78 \times 10^{-13}$  cm.

It is important to note that the function  $P_{\text{abs}}(r)$  is effectively unchanged by variation within a wide range of the initial distribution over  $l$  of the pions captured by the Coulomb potential of the nucleus. In other words,

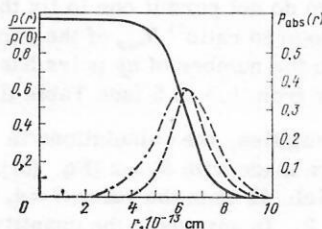


FIG. 1. Distributions of the density  $\rho(r)/\rho_0$  of nuclear matter (left-hand scale) and the probability of absorption  $P_{\text{abs}}(r)$  (right-hand scale) for the nucleus  $^{181}\text{Ta}$ . The continuous curve is a calculation of  $\rho(r)/\rho_0$  in accordance with Eq. (3); the broken curve, the calculation of  $P_{\text{abs}}(r)$  from Ref. 44; the chain curve, the calculation of  $P_{\text{abs}}(r)$  in accordance with Eq. (2) with  $\Delta r = 0$ .

the effects of the valence electrons ignored in Ref. 44 and the other fine details of the interaction of the pion with the electron shell of the atom in the initial stage of the transition of the pion from the continuum to the discrete spectrum cannot change the conclusion that the pion is absorbed in the surface layer.

This important aspect of the process—the surface nature of the absorption—is taken into account only in the models proposed in Refs. 40 and 44.

*Absorption of the Pion by the Nucleus.* We now consider the actual process of absorption of the pion by the nucleus. It is generally assumed that the pion is basically absorbed by a pair of nucleons. The  $\pi^-$  meson can be absorbed by an  $np$  or a  $pp$  pair:



In the simplest case, if spin effects are ignored, the charge state of the two nucleons that absorb the pion is determined by the number of pairs of the given type, and then the probability of absorption by an  $np$  pair is

$$W_{np} = NZ / [NZ + Z(Z-1)/2], \quad (5)$$

where  $N$  is the number of neutrons and  $Z$  the number of protons in the nucleus. It follows from (5) that the pion must be absorbed more often by an  $np$  pair than by a  $pp$  pair:

$$R = W_{np} / W_{pp} = 2N / (Z-1) > 1.$$

For example, for the  $^{208}\text{Pb}$  nucleus  $R = 3.1$ .

The influence of the isospin on the ratio of the probabilities of pion absorption by  $np$  and  $pp$  pairs was investigated in Ref. 44. The ratio  $R$  can be expressed in terms of the amplitudes of pion absorption  $f_{TI}$  ( $T$  is the isospin of the two nucleons and  $I$  is the total isospin of the pion and nucleons) as follows:

$$R = R_0 N / (Z-1), \quad (6a)$$

where

$$R_0 = 3(2|f_{01}|^2 + |f_{11}|^2) / (2|f_{01}|^2 + 3|f_{11}|^2). \quad (6b)$$

If the absorption occurs through a partial wave with isospin  $3/2$ , then  $R_0 = 5$ . In the case of absorption through a partial wave with isospin  $1/2$ , the value of  $R_0$  can vary from 0 to 2. This range of variation is typical of various theoretical estimates. At the present time, the experimental data also do not permit one to fix the value of  $R$ , since the measured ratio<sup>1)</sup>  $R_{\text{exp}}$  of the number of emitted  $m$  pairs to the number of  $np$  pairs has a large error and may vary from 1.5 to 5 (see Table II).

Because of these uncertainties, the calculations in Refs. 39, 40, and 44 were made with  $R_0 = 2$  [Eq. (5)]. The model described in Ref. 42 uses the value  $R = 4$ , which is taken from Ref. 2. In any case, the quantity  $R$  must at present be regarded as a parameter whose value is found by matching to the experiments.

<sup>1)</sup>  $R_{\text{exp}} < R$  because of the possibility that a nucleon leaving the nucleus is scattered with charge exchange.

After absorption by the pair of nucleons, the pion mass  $m_\pi$  is realized in the form of kinetic energy of secondary nucleons, each of which will have in the center-of-mass frame the energy  $T = m_\pi/2$ . In the center-of-mass frame, the secondary nucleons are emitted isotropically in opposite directions. In the laboratory frame, because of the momenta of the intranuclear nucleons, the energies of the secondary particles will have a definite spread around the value  $m_\pi/2$ . The models described in Refs. 39, 40, and 44 take into account the "smearing" over the momenta of the nucleon pairs in the nucleus: The momentum of the pair is equal to the sum of the momenta of two intranuclear nucleons, which are determined from the corresponding Fermi distribution. In the model considered in Ref. 42 this "smearing" effect is not taken into account.

*Multiscattering and Absorption in the Nucleus of the Fast Nucleons.* Thus, as a result of absorption of the pion in the diffuse layer of the nucleus two nucleons are formed with energy 50–100 MeV. Depending on the direction of their motion and the point of absorption of the pion, the nucleons may leave the nucleus without interaction or undergo one or several collisions with intranuclear nucleons. This stage of the process is analogous to an ordinary nuclear reaction in which a nucleon of medium energy incident on a nucleus initiates an intranuclear cascade in the nucleus.

For such processes, the papers of Refs. 39, 40, and 44 use a model of intranuclear cascades that gives a fairly good description of reactions initiated by nucleons with energy  $\sim 100$  MeV (see, for example, the review of Ref. 47). It should be noted that here no additional parameters are introduced, since all the parameters of the cascade model are determined independently by an analysis of the nucleon–nucleus interactions. A detailed description of the model of intranuclear cascades can be found in Ref. 47, and therefore it is here meaningful to give only a brief review of its main propositions. In the model, the interaction of a nucleon with the nucleus reduces to a series of successive nucleon–nucleon collisions. The nucleus is regarded as a degenerate Fermi gas of free nucleons in a spherical potential well. The density distribution of the intranuclear nucleons is taken in the form (3).

In Ref. 42, two "parallel" intranuclear cascades are described by means of the exciton model (see the review of Ref. 48). One of the difficulties of this model in a calculation of ordinary nuclear reactions resides in the choice of the initial configuration of the system, i.e., the number of particles  $p$  and holes  $h$ . Ultimately, the configuration is varied in order to obtain best agreement with the experiments. In Ref. 42, the initial configuration  $1p-1h$  with energy 70 MeV was taken for each of the cascades. The subsequent competition between the different decay modes of the intermediate system in the cascade process is determined by the partial widths for emission of particles and the exciton–exciton interaction, the details of the calculation of these being given in Ref. 49.

*Establishment of Statistical Equilibrium in the Residual Nuclei.* After the intranuclear cascade has ended in



the degenerate Fermi gas as a result of collisions of the cascade particles with the intranuclear nucleons, holes are formed. In addition, some of the cascade nucleons are unable to overcome the nuclear potential and are in a bound state in levels above the Fermi energy. The resulting system is not in equilibrium. In the passage to the following, "evaporation" stage of the process, particles can be emitted from the residual nucleus.

To estimate the part played by pre-equilibrium emission, the exciton model of Ref. 48 was chosen in Ref. 40. The doorway state for the exciton model is determined by the previous stage of multiple scattering of fast nucleons. The actual calculations of the establishment of equilibrium are made by means of the modified exciton model described in Refs. 50 and 51.

As a rule, the influence of pre-equilibrium emission of particles on the global characteristics of the process of pion absorption by nuclei is small,<sup>40</sup> so that in a first approximation it can be ignored in the models of Refs. 39, 40, and 44. However, in some phenomena the pre-equilibrium processes can be manifested fairly strongly, and in this case a correct treatment of the thermalization of the residual nucleus is necessary.

With regard to the model of Ref. 42, the thermalization stage is taken into account automatically through the exciton formalism chosen to describe the nuclear reaction.

*Emission of Particles and Fission of the Highly Excited Nucleus.* After establishment of thermodynamic equilibrium, the highly excited residual nucleus "evaporates" particles successively or undergoes fission. The process of de-excitation and fission of the residual nucleus proceeds in the same way as in an ordinary compound nucleus formed in reactions with low-energy particles or with heavy ions.<sup>21</sup> For the description of this process, one usually uses the statistical model of Weisskopf<sup>52</sup> for the emission of particles and the Bohr-Wheeler<sup>53</sup> model for the fission.

In Refs. 39, 40, 42, and 44, actual calculations of the de-excitation of compound nuclei were made by means of the method developed in Refs. 54 and 55. The Fermi-gas dependence of the level density of the nucleus on its excitation energy  $E^*$  was used:

$$\rho(E^*) \sim \exp(2\sqrt{aAE^*}), \quad (7)$$

where  $a \approx 0.1 \text{ MeV}^{-1}$  is the level-density parameter, and  $A = Z + N$ . The calculations take into account the possibility of emission of six species of particle:  $n$ ,  $p$ ,  $d$ ,  $t$ ,  $^3\text{He}$ , and  $\alpha$ . The method of Refs. 54 and 55 is generalized to the case of fission in Ref. 56.

Thus, the process of absorption of a stopped  $\pi^-$  meson has a complicated and many-sided nature, combining both features of low-energy nuclear reactions as well as reactions initiated by particles of medium energy. Therefore, the Monte Carlo method was chosen as the method of calculation in Refs. 39, 40, 42, and 44.

<sup>21</sup>By compound nucleus, we shall understand a residual nucleus in which thermodynamic equilibrium has been established.

Compared with analytical methods, this method has an obvious shortcoming due to the need for a computer. However, this shortcoming is offset by the possibility of calculating, in the framework of a single approach, the most varied characteristics of the process associated with not only the emission of secondary particles (the products of many-nucleon absorption of the pions) but also the properties of the resulting residual nucleus.

Before we turn to the experimental investigations, let us describe briefly the existing theoretical approaches. One of them<sup>39,40,44</sup> is based on the use of the model of intranuclear cascades to describe the second stage of the process, while the other<sup>42</sup> is based on the exciton model. At the present time, the first approach evidently has greater potential possibilities, since, in contrast to the exciton approach, it permits one to calculate characteristics in which the surface nature of pion absorption by nuclei is most clearly manifested, for example, the high spin of the residual nuclei and the various correlations of the emitted high-energy particles.

## 2. EMISSION OF PARTICLES BY THE EXCITED NUCLEUS

*Energy Spectra of the Neutrons.* An important type of decay of the highly excited complex nucleus after absorption of a  $\pi^-$  meson is the emission of neutrons. The most detailed information about such neutrons is obtained in experiments in which their energy spectra are measured.<sup>18-20,57</sup>

In Fig. 2, we show the neutron spectrum obtained in the case of absorption of slow  $\pi^-$  mesons by  $^{59}\text{Co}$  and  $^{197}\text{Au}$  nuclei. The spectrum has the characteristic feature associated with the existence of the cascade and evaporation stages in the process of  $\pi^-$  absorption. The spectrum clearly reveals two components consisting of evaporation and fast neutrons. In the evaporation part of the spectrum we have neutrons emitted by excited residual nuclei, whereas the high-energy part of the spectrum is formed by fast cascade particles emitted from the surface layer of the nucleus virtually without collisions with intranuclear nucleons.

A consequence of the surface nature of the absorption

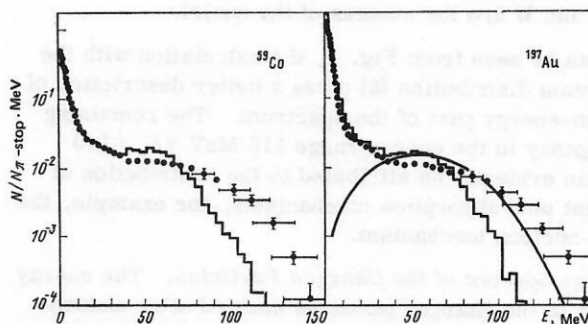


FIG. 2. Energy spectra of neutrons after absorption of slow  $\pi^-$  by  $^{59}\text{Co}$  and  $^{197}\text{Au}$  nuclei. The black circles are the experiment of Ref. 57, the histograms the calculation from Ref. 58, and the curve is the calculation from Ref. 59;  $N/N_{\pi\text{-stop}}$  is the number of counts normalized by the number of stopped  $\pi^-$  mesons in a definite energy range.



is the circumstance that the high-energy part of the spectrum depends weakly on the atomic number of the target nucleus—both in form and in magnitude (see Fig. 2). Therefore, the mean multiplicity  $\bar{\nu}_n$  of the fast neutrons is also virtually independent of  $A$ , and the experimental values of  $\bar{\nu}_n$  for the nuclei  $^{59}\text{Co}$  and  $^{197}\text{Au}$  are, respectively, 1.38 and 1.32 neutrons per absorbed pion.<sup>57</sup> The increase in the total multiplicity from 4.04 neutrons for the  $^{59}\text{Co}$  nucleus to 6.31 neutrons for the  $^{197}\text{Au}$  nucleus indicates a strong dependence of the multiplicity of the evaporation neutrons on the mass of the target nucleus, which is a reflection of the growth in the excitation energy of the residual nuclei.

The theory of Refs. 40 and 58 gives a good description of the evaporation part of the spectrum. However, the fast component of the spectrum is significantly softer than the experimental spectrum, and although the maximum of this part of the spectrum is at the energy  $E \approx m_\pi/2 - B_n \approx 60$  MeV ( $B_n$  is the nucleon binding energy), its smearing in the region of high energies is clearly insufficient. This evidently indicates an incorrect description in Refs. 39, 40, and 44 of the high-momentum component in the distribution of intranuclear nucleons. The local-density approximation used in these papers leads to low momenta of the nucleons of the nucleus on its periphery and, therefore, to a small smearing of the neutron spectrum.

This is confirmed by a simplified calculation<sup>59</sup> of the fast component of the neutron spectrum made under the assumption that one of the neutrons produced in the reaction (4a) emerges from the nucleus without interaction with it, while the other is absorbed by the nucleus. If the momentum distribution of the intranuclear nucleons is taken in the form

$$f(P) \sim \exp(-P^2/\alpha^2), \quad (8)$$

where the parameter  $\alpha$  has a value in the range 13 MeV  $\leq \alpha^2/2m_N \leq 20$  MeV, the expression for the neutron spectrum can be written in the form

$$dN/dE_n \sim \sqrt{E_n(E_0 - E_n)} \exp[-(m_N/\alpha^2)(\sqrt{E_n} - \sqrt{E_0 - E_n})^2]. \quad (9)$$

Here,  $E_0 = m_\pi - B_\pi + M(A, Z) - M(A, Z-1) - B_{2N}$ ,  $m_N$  is the nucleon mass,  $B_\pi$  is the pion binding energy,  $B_{2N}$  is the binding energy of two nucleons in the  $(A, Z-1)$  nucleus, and  $M$  are the masses of the nuclei.

As can be seen from Fig. 2, the calculation with the momentum distribution (8) gives a better description of the high-energy part of the spectrum. The remaining discrepancy in the energy range 110 MeV  $\leq E_n \leq 140$  MeV can evidently be attributed to the contribution of different pion absorption mechanisms, for example, the single-nucleon mechanism.

**Energy Spectra of the Charged Particles.** The energy spectra of the charged particles emitted after absorption of stopped  $\pi^-$  mesons by different nuclei were measured in Refs. 60–66. In Figs. 3a and 3b, we show the experimental spectra of protons, deuterons, tritons, helium-3, and  $\alpha$  particles taken from Refs. 64 and 66.

All that we have said earlier concerning the neutron spectra remains valid for the proton spectra, except

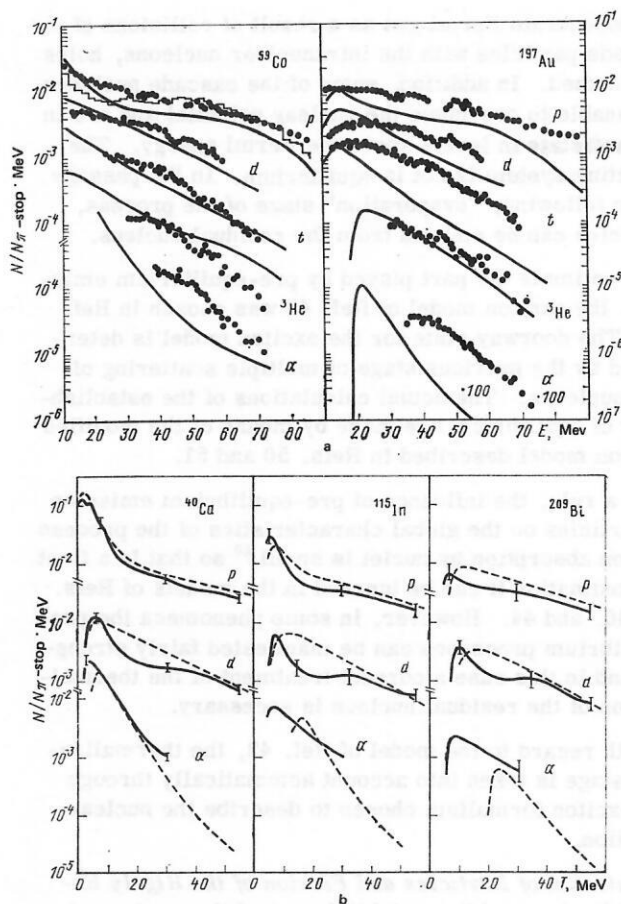


FIG. 3. Energy spectra of  $p$ ,  $d$ ,  $t$ ,  $^3\text{He}$ , and  $\alpha$  emitted by the nuclei  $^{59}\text{Co}$  and  $^{197}\text{Au}$  (a) and  $\text{Ca}$ ,  $\text{In}$ , and  $\text{Bi}$  (b) after absorption of slow  $\pi^-$  mesons. a) The black circles are the results of the experiment of Ref. 64, the continuous curve the calculation of Refs. 58 and 67, and the histogram the calculation of Refs. 42 and 77; b) the continuous curve gives the results of the experiment of Ref. 66 and the broken curve the results of the calculation in Ref. 58.

that in the case of heavy nuclei the evaporation component of the proton spectrum is not clearly expressed because of the influence of the Coulomb barrier. The fast component of the proton spectrum is formed by the reaction (4b), and therefore at an energy above 70 MeV, as in the case of neutrons, the calculation of Ref. 58 gives a softer spectrum because of the small amount of smearing over the momenta of the intranuclear nucleons.

Figure 3 also shows the proton spectrum calculated in the framework of the model described in Ref. 42. The spectrum is taken from the later paper of Ref. 64. To extend the proton spectrum calculated in the exciton model to the region  $E_n > 60$  MeV, it was necessary to take into account the smearing with respect to the Fermi momentum for the intranuclear nucleons.

Comparison of the calculated neutron and proton spectra with the experiments shows that at an energy  $\sim 60$  MeV, which corresponds to the maximum of the fast component, the neutron spectrum is 1.5 times higher and the proton spectrum is 1.5 times lower than the experimental spectrum. Clearly, this indicates a need to

choose a value of  $R$  in the calculations of Refs. 40 and 44 that is smaller than the one given by Eq. (5).

Of great interest to investigators is a measurement of the spectra of complex charged particles, since it is usually assumed that such particles can be formed as a result of many-nucleon absorption of pions. However, before we investigate this question in the case of complex nuclei, it is necessary to elucidate the contribution of other possible mechanisms to the production of these particles.

The simplest such mechanism is the evaporation mechanism, in which the charged particle is emitted by a highly excited compound nucleus. The calculations made in Ref. 67 showed that in this case one cannot reproduce either the form or the absolute magnitude of the spectra shown in Fig. 3.

In Ref. 67, it is shown that an important contribution to the spectra of complex charged particles is made by pre-equilibrium processes. If one does not assume the existence of complex particles, or clusters, already "prepared" in the nucleus, the rate of emission of pre-equilibrium particles of species  $\beta$  with energy  $\varepsilon$  from the state of a nucleus with excitation energy  $E^*$  and number  $n = p + h$  of excited particles and holes can be written in the form<sup>68</sup>

$$= \left[ \gamma_{\beta} R_{\beta}(p) \frac{W_{\beta}(p, h, E^*, \varepsilon) d\varepsilon}{\omega(p - p_{\beta}, h, E^* - B_{\beta} - \varepsilon) \omega(p_{\beta}, 0, B_{\beta} + \varepsilon)} \right] \times \frac{(2s_{\beta} + 1)}{\pi^2 \hbar^3} \frac{m_{\beta} \varepsilon \sigma_{\text{inv}}}{g} d\varepsilon. \quad (10)$$

Here,  $s_{\beta}$ ,  $m_{\beta}$ ,  $B_{\beta}$ , and  $\sigma_{\text{inv}}$  are the spin, mass, binding energy, and cross section of the inverse reaction for the emitted particle;  $\omega$  is the density of particle-hole states; and  $g$  is the density of single-particle states in the approximation of an equidistant spectrum. The factor  $R_{\beta}(p)$  determines the correct isotopic composition, and the parameter  $\gamma_{\beta}$  describes the probability  $p_{\beta}$  of grouping of nucleons into the complex particle. If  $\gamma_{\beta}$  is determined as the overlap integral of the wave functions  $\psi_i$  of independent nucleons with the cluster wave function  $\psi_{\beta}$ , a very simple estimate gives

$$\gamma_{\beta} = \left| \int \psi_i \dots \psi_{p_{\beta}} \psi_{\beta}^* d\mathbf{x}_1 \dots d\mathbf{x}_{p_{\beta}} \right|^2 \approx p_{\beta}^3 (p_{\beta}/A)^{p_{\beta}-1}. \quad (11)$$

As can be seen in Fig. 3, the contribution of the pre-equilibrium particles in the spectra is very large. At the same time, in the region of high energies the calculation is as a rule below the experiment (see Fig. 3a). It is possible that the discrepancy in this region could be eliminated either by the mechanism of emission after many-nucleon absorption of the pion noted above or by the mechanism of emission of complex particles during the stage of the intranuclear cascade. Among these last processes, we can include the process of capture of an intranuclear nucleon by a fast nucleon and also the knockout by fast nucleons of clusters already prepared in the nucleus. Hitherto, the contribution of such mechanisms has not been taken into account in the models of Refs. 39, 40, and 42.

It should be noted that the mechanisms of emission of complex charged particles considered here (pre-equilibrium

emission, capture, and knockout) must also be present in the case of inelastic proton-nucleus interaction at energy  $E_p \approx m_{\pi}/2$ . Therefore, to determine the fraction of charged particles emitted as a result of pion absorption by many-nucleon associations, it is expedient to use in the analysis the results of proton-nucleus experiments. For example, experiments made at the proton energies  $E_p = 62$  MeV (Ref. 79), 72 MeV (Ref. 169), and 90 MeV (Ref. 94) showed that the spectra of  $d$ ,  $t$ ,  $^3\text{He}$ , and  $\alpha$  particles in proton- and pion-nucleus interactions have a similar form. This indicates that secondary processes make a large contribution to the emission of complex particles.

**Correlations of the Emitted Particles.** Valuable information about the mechanism of pion absorption by nuclei has also been obtained in experiments that measured the energy and angular distributions of various particles in coincidence.<sup>57, 69-76</sup> The angular correlations of two neutrons or a neutron and a proton have a sharp peak at angle  $180^\circ$  for the carbon nucleus, this peak becoming broader on the transition to the heavier nuclei  $^{59}\text{Co}$  and  $^{197}\text{Au}$  (Fig. 4). Such a picture corresponds to the two-nucleon mechanism of pion absorption and cannot be well described in the approach based on the model of intranuclear cascades.<sup>39</sup> The energy spectrum of one neutron in coincidence with another neutron<sup>57</sup> has a broad maximum for the  $^{12}\text{C}$  nucleus at energy 50-60 MeV (Fig. 5), which is a further indication of the two-nucleon absorption mechanism. In the kinematically complete experiments for the  $(\pi^-, 2n)$  reaction on the nuclei  $^9\text{Be}$ ,  $^{10}\text{B}$ ,  $^{12}\text{C}$ ,  $^{14}\text{C}$ ,  $^{40}\text{Ca}$  (Refs. 74-76) it proved possible not only to prove the predominant part played by the two-particle absorption mechanism but also to obtain information about the state of the absorbing nucleon pair. For example, in Ref. 75 it was shown that the pion is absorbed preferentially by a pair of nucleons that are in the  $1s$  relative state.

Recently, an experiment was made at SIN in which a measurement was made of the angular correlations for charged particles<sup>73</sup> emitted after  $\pi^-$  absorption in  $^{12}\text{C}$

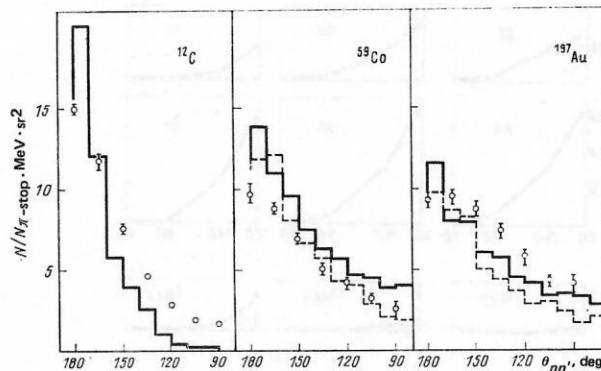


FIG. 4. Angular correlation of two neutrons detected in coincidence after  $\pi^-$  absorption by  $^{12}\text{C}$ ,  $^{59}\text{Co}$ , and  $^{197}\text{Au}$  with the neutron detection threshold  $E_n = 20$  MeV. The open circles are the data of Ref. 57; for  $^{12}\text{C}$  the continuous line gives the results of the calculation in Ref. 39; for  $^{59}\text{Co}$  and  $^{197}\text{Au}$  the continuous line gives the results of the calculation in Ref. 58 with allowance for pre-equilibrium emission of particles and the broken curve is without allowance for them.

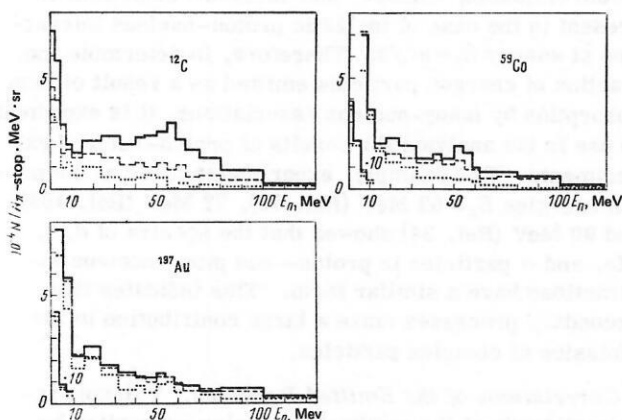


FIG. 5. Energy spectra of correlated neutrons at the angle  $\theta_{nn}=180^\circ$  (continuous line),  $150^\circ$  (broken line), and  $120^\circ$  (dotted line) in the case of  $\pi^-$  absorption.<sup>57</sup> The energy of the second neutron in the experiment of Ref. 57 must exceed 20 MeV.

(Fig. 6). Measurements were made of the correlations for the following pairs:  $pp, pd, dd, pt, tt, {}^3\text{He}p, \alpha p, {}^3\text{He}d, \alpha d, {}^3\text{He}t, \alpha t$ . Unfortunately, these data have not yet been analyzed theoretically. For the moment, all one can say is that the distribution with respect to the emission angle is much narrower than for isotropic uncorrelated particle emission. This indicates that a contribution is made to the process of emission of complex charged particles by mechanisms such as many-nucleon pion absorption by associations, the knocking out of particles by cascade nucleons, and the capture of nucleons.

### 3. PROPERTIES OF THE RESIDUAL NUCLEI FORMED AFTER ABSORPTION OF SLOW $\pi^-$ MESONS

**Isotope Yields.** Another important characteristic of the absorption of  $\pi^-$  mesons by nuclei, and it has been studied in many experiments (Refs. 22–24, 34–38, 44, 73, 77, 78, 80–88, 91, and 92), is the yield of isotopes.

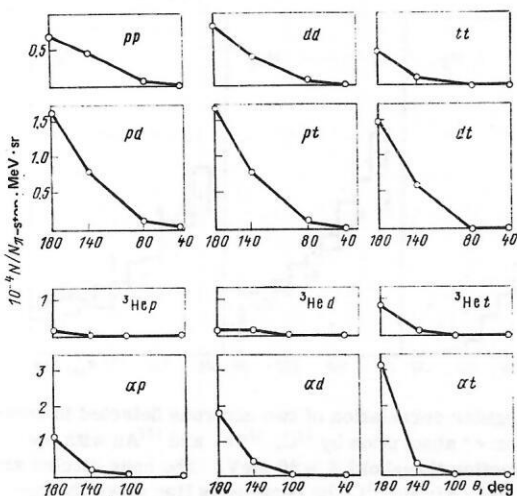


FIG. 6. Distributions with respect to the emission angle for different pairs of charged particles resulting from the absorption of slow  $\pi^-$  mesons by  ${}^{12}\text{C}$  (Ref. 73). The energy threshold is 20 MeV for the hydrogen isotopes and 30 MeV for the helium isotopes.

Experiments on the isotope yields by means of the so-called activation method are fairly simple in their realization and are based on detection of  $\gamma$  rays from the residual nuclear products formed after  $\pi^-$  absorption by the target nucleus. The scheme of target irradiation used in the Dubna experiments is shown in Fig. 7a. Protons with energy  $E_p \approx 670$  MeV and intensity  $1.5 \times 10^{12} \text{ sec}^{-1}$  are focused by a system of quadrupole lenses on a copper target, which is a copious source of slow  $\pi^-$  mesons. The pions with energy  $E_\pi \approx 30$  MeV are focused by a wide-angle solenoidal magnetic lens on the investigated target. The density of stoppings in the target reaches  $\sim 2 \times 10^4 \text{ g}^{-1} \cdot \text{sec}^{-1}$  (Ref. 89). The times of irradiation, "cooling," and measurement of the targets were varied, depending on the half-life of the expected nuclear products. The  $\gamma$ -ray spectra were measured by means of Ge (Li) detectors of various volumes. In individual cases, to achieve clean separation of the investigated isotopes, radiochemical separation was used. Such a method makes it possible to identify not only short-lived isotopes with half-life up to 30 sec (without the use of radiochemistry) but also long-lived isotopes with periods up to 100 h. During the experiment, all the accumulated  $\gamma$ -ray spectra were fed into a computer, in which they were then processed by standard codes.

In the experiments at the meson factories at SIN and

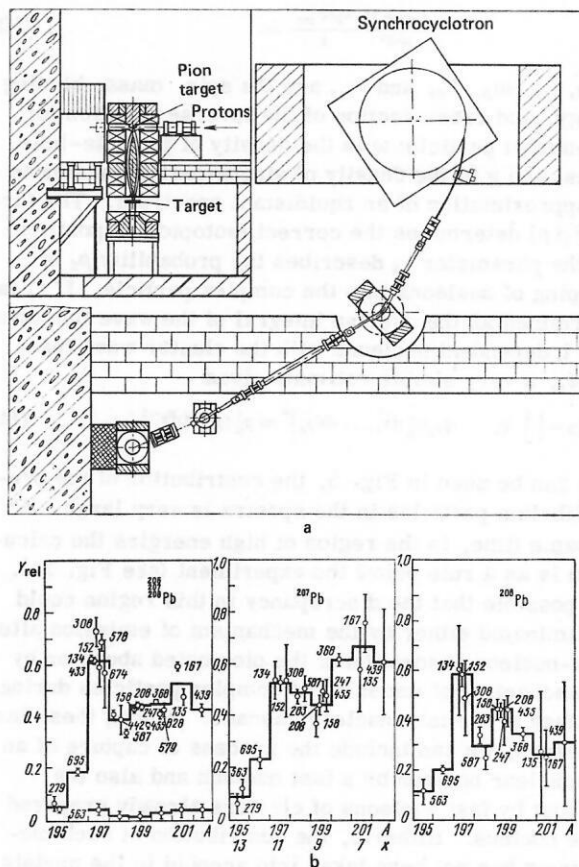


FIG. 7. Arrangement of experiment to investigate the mechanism of negative pion capture (a) and the yield of thallium isotopes produced by the capture of  $\pi^-$  by lead nuclei<sup>85</sup> in relative units (b). The numbers are the energies of the  $\gamma$  lines of the produced thallium isotopes.



CERN the spectra of prompt  $\gamma$  rays resulting from the irradiation of targets directly in a  $\pi^-$  beam are investigated. Simultaneously, there is a possibility of measuring the spectra of the neutrons and the charged particles  $p$ ,  $d$ ,  $^3\text{H}$ , and  $^3\text{He}$ . The density of  $\pi^-$  stoppings in the target is also  $2 \times 10^4 \text{ g}^{-1} \cdot \text{sec}^{-1}$  (Ref. 64).

Each of these methods has its advantages and disadvantages, but the important thing is that they are simple to realize and make it possible to obtain new information on the mechanism of  $\pi^-$  absorption by nuclei.

Already in the first experiments of this type<sup>35</sup> based on detection of the  $\gamma$  rays of the product nucleus after  $\pi^-$  absorption by  $^{206-208}\text{Pb}$  nuclei it was shown that the distribution with respect to the number of emitted particles is not narrow (3–4 particles), as in reactions with low-energy particles, but broad, varying in the range from 2 to 16 particles (Fig. 7b), and that in the case of emission of between 2 and 16 neutrons their total kinetic energy lies in the range from 120 to 1 MeV.

The broad distribution with respect to the number of emitted particles in the case of absorption of slow  $\pi^-$  mesons can be explained simply in the models described in Refs. 39, 40, and 44. Since the energy of the cascade particles varies in a fairly wide range (see Fig. 2), the distribution of the residual nuclei with respect to the excitation energy will also be broad. In this approach, the excitation energy of the nucleus is the sum of the energies of the particles and the holes measured from the Fermi energy. Then from the energy balance, we obtain

$$E^* \approx m_\pi - \sum_i (E_i + \bar{B}_N), \quad (12)$$

where  $E_i$  is the kinetic energy of the  $i$ th cascade nucleon in the laboratory frame, and  $\bar{B}_N = 7 \text{ MeV}$  is the mean nucleon binding energy in the nucleus.

In Fig. 8, as an example, we show the distribution with respect to the excitation energy of the residual nuclei before the evaporation stage. For the heavy nucleus Pb, the excitation energy varies in a wide range, from a few MeV to 140 MeV, which corresponds to complete absorption of all the cascade particles and transformation of the entire pion mass into the excitation energy of the nucleus. For a light nucleus, the  $E^*$  distribution is narrower and its maximum is shifted to lower  $E^*$ .

The mean excitation energy increases with increasing mass number  $A$  of the target nucleus (Fig. 9). Therefore, the heavier the target nucleus, the broader is the

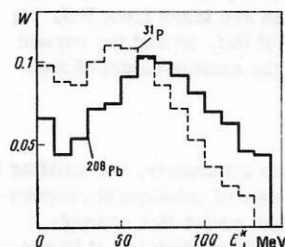


FIG. 8. Distribution with respect to the excitation energy  $E^*$  of the residual nuclei produced after absorption of  $\pi^-$  mesons.

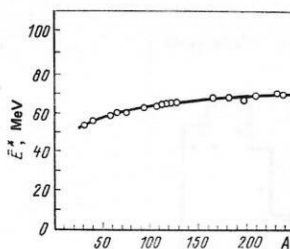


FIG. 9. Dependence of the mean excitation energy  $\bar{E}^*$  of residual nuclei in  $\pi^-$  capture reactions on the mass number of the target nucleus. The curve drawn through the points is the calculation of Ref. 58.

curve of the isotope yield. Usually, the experimental isotope-yield curves are approximated by Gaussian curves. Such an approximation of the data made in Ref. 77 by various authors for  $^{62}\text{Ni}$ ,  $^{127}\text{I}$ ,  $^{133}\text{Cs}$ ,  $^{165}\text{Ho}$ ,  $^{175}\text{Lu}$ ,  $^{208}\text{Pb}$ ,  $^{59}\text{Co}$ ,  $^{75}\text{As}$ ,  $^{197}\text{Au}$ ,  $^{209}\text{Bi}$  targets does indeed show that the width at half-height of the Gaussian curve increases strongly on the transition to the heavier nuclei (Fig. 10).

In Figs. 11–14, we compare the experimental yields of the reactions  $(\pi^-; \gamma p, xn)$  on the nuclei  $^{31}\text{P}$ ,  $^{59}\text{Co}$ ,  $^{181}\text{Ta}$ ,  $^{197}\text{Au}$  with calculations made with different models<sup>40,42,44</sup> for the description of pion absorption by complex nuclei. The existing models reproduce equally well the main features of the disintegration of the nuclei after  $\pi^-$  absorption. This can evidently be attributed to the major part played by the evaporation stage in the formation of the given final isotope, this being present in all models and, moreover, described in the same way. It is therefore natural that the differences between the different models must be most strongly reflected in the yields of reactions with emission of a small number of particles. In the approaches of Refs. 40 and 44, which take into account the surface nature of the absorption, these yields must exceed the yield calculated in the exciton model.<sup>42</sup> In the case of the  $(\pi^-, xn)$  reaction, the calculations for the heavy nuclei in accordance with the cascade-evaporation model<sup>40,44</sup> are lower than the experimental values at large  $x > 12$ . As is shown in Ref. 40, this may indicate a possible contribution of the  $\alpha$ -particle absorption mechanism.

In the case of light and medium targets, emission of charged particles makes a large contribution to the for-

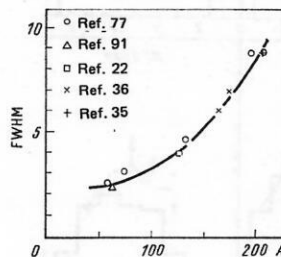


FIG. 10. Dependence on the mass number  $A$  of the full width at half height (FWHM) of the isotope-yield curves in the case of absorption of  $\pi^-$  mesons by the following targets:  $^{59}\text{Co}$  (Ref. 77),  $^{62}\text{Ni}$  (Ref. 91),  $^{75}\text{As}$  (Ref. 77),  $^{127}\text{I}$  (Ref. 22),  $^{133}\text{Cs}$  (Ref. 77),  $^{165}\text{Ho}$  (Ref. 36),  $^{175}\text{Lu}$  (Ref. 36),  $^{197}\text{Au}$  (Ref. 77),  $^{208}\text{Pb}$  (Ref. 35),  $^{209}\text{Bi}$  (Ref. 77) (approximated in Ref. 77 by Gaussian curves).

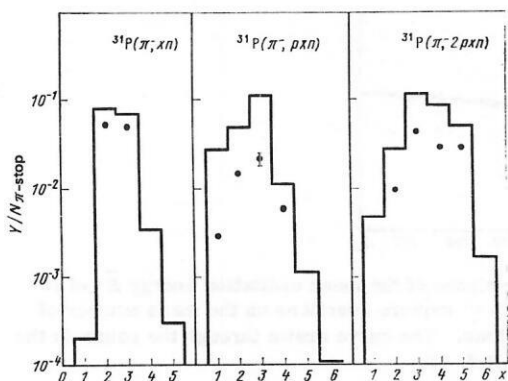


FIG. 11. Yield of isotopes after absorption of  $\pi^-$  mesons by  $^{31}\text{P}$  nuclei. The black circles are from the experiment in Ref. 38, the histograms the calculation in Ref. 58.

mation of the final isotope (Table I). In heavy nuclei, the high Coulomb barrier hinders the emission of charged particles in the final stages of the process, and here the  $(\pi^-, xn)$  reaction predominates over all other reactions. In accordance with the expression (5), the yield of the  $(\pi^-, pxn)$  reaction in the region of heavy nuclei will be smaller than the yield of the  $(\pi^-, xn)$  reaction, since the Coulomb barrier does not have a significant influence on the emission of a fast proton resulting from absorption of a pion by a  $pp$  pair. Therefore, one can in principle extract information about the ratio  $R = W_{np}/W_{pp}$  from the ratio of the yields of the  $xn$  and  $pxn$  reactions on heavy nuclei.

In particular, one of the experimental ways of obtaining information about  $R$  can be through measurement of the isobar ratio. This is the ratio of the independent yields (production cross sections) of the two isobar nuclei. The values of the isobar ratio, determined from the two isobar nuclei  $^{159}\text{Er}$  and  $^{159}\text{Ho}$  in the  $^{169}\text{Tm}(\pi^-, 10n)$

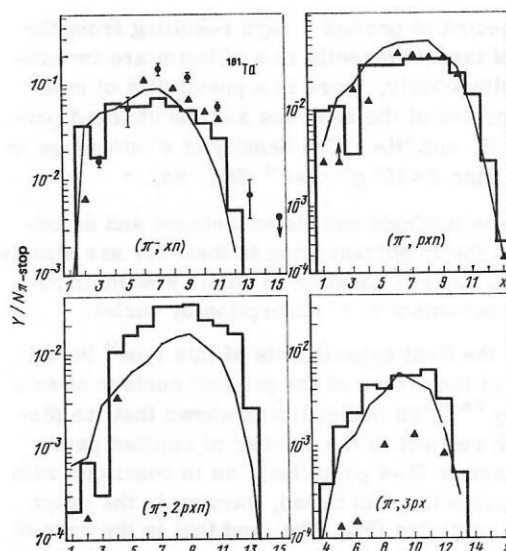


FIG. 13. Yield of isotopes after absorption of  $\pi^-$  mesons by  $^{181}\text{Ta}$  nuclei. The experimental data are taken from Ref. 44 (black triangles) and Ref. 88 (black circles); the histograms are the calculation of Ref. 58 and the curves the calculation of Ref. 44.

and  $^{169}\text{Tm}(\pi^-, p9n)$  reactions, and also for the nuclei  $^{200}\text{Pb}$  and  $^{200}\text{Tl}$  in the  $^{209}\text{Bi}(\pi^-, 9n)$  and  $^{209}\text{Bi}(\pi^-, p8n)$  reactions, are, respectively,  $I = \sigma_1/\sigma_2 = 9.8 \pm 2.3$  (ref. 86) and  $I = \sigma_1/\sigma_2 = 11.0 \pm 5.6$  (Ref. 85). To relate these isobar ratios to the probability of pion absorption by  $np$  and  $pp$  pairs, let us consider the main channels leading to the production of these isobar nuclei. The isotopes  $^{159}\text{Er}$  and  $^{200}\text{Pb}$  can be produced in the processes  $\pi^- pp \rightarrow pn$  with subsequent absorption of a proton and  $\pi^- np \rightarrow nn$  with absorption of a neutron, and the isotopes  $^{159}\text{Ho}$  and  $^{200}\text{Tl}$  can be produced only in the process  $\pi^- pp \rightarrow np$  with absorption of a neutron.<sup>3)</sup> Then we obtain  $R = (I - 1)/2$ , where  $I$  is the experimentally obtained isobar ratio. In accordance with this last formula,  $R = 4.4 \pm 1.1$  for  $^{169}\text{Tm}$  and  $R = 5.0 \pm 2.8$  for  $^{209}\text{Bi}$ . These

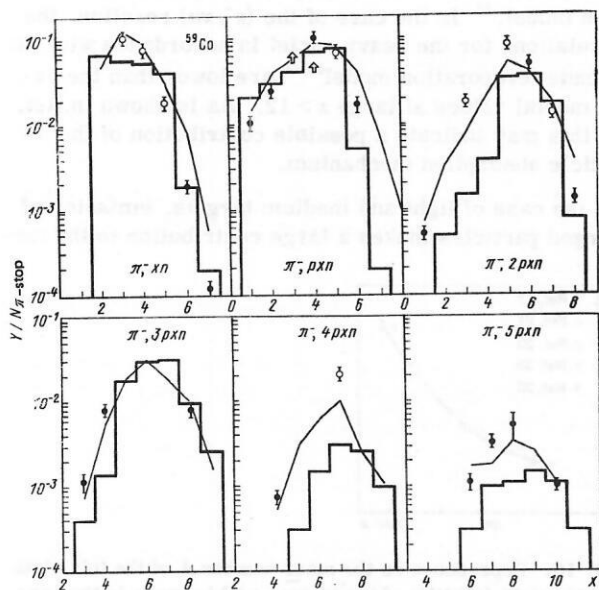


FIG. 12. Yield of isotopes after absorption of  $\pi^-$  mesons by  $^{59}\text{Co}$  nuclei. The experimental data are taken from Ref. 77, the histograms are calculated in accordance with the cascade-evaporation model of Ref. 58, and the curves are calculated with the exciton model of Ref. 77.

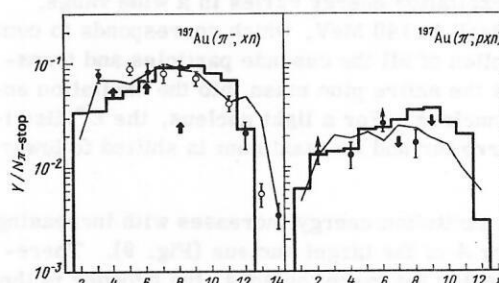


FIG. 14. Yield of isotopes after absorption of  $\pi^-$  mesons by  $^{197}\text{Au}$  nuclei. The experimental data are taken from Ref. 77; the histograms are the calculation of Ref. 58 and the curves the calculation in accordance with the exciton model of Ref. 77.

<sup>3)</sup> The value of  $R$  is determined more accurately, the smaller is the difference between the processes of subsequent evaporation of the neutrons from the isobar nuclei (for example,  $^{159}\text{Er}$  and  $^{159}\text{Ho}$  or  $^{200}\text{Tl}$  and  $^{200}\text{Pb}$ ). In particular, it is necessary that the sums of the binding energies  $B_n$  of the neutrons emitted by the compound nuclei be nearly equal.

TABLE I. Experimental and theoretical yields (%) of different reaction channels in the case of absorption of stopped  $\pi^-$  mesons by  $^{59}\text{Co}$  and  $^{197}\text{Au}$  nuclei.

Reaction	$^{59}\text{Co}$			$^{197}\text{Au}$		
	Experiment (Ref. 77)	Calculation (Ref. 58)	Calculation (Ref. 77)	Experiment (Ref. 77)	Calculation (Ref. 58)	Calculation (Ref. 77)
$(\pi^-, \pi n)$	$24 \pm 3$	23.2	34.0	$74 \pm 8$	69.0	76.3
$(\pi^-, p \pi n)$	$32 \pm 3$	25.4	35.9	$20 \pm 7$	23.6	18.9
$(\pi^-, 2p \pi n)$	$24 \pm 3$	30.9	16.1	—	—	—
$(\pi^-, 3p \pi n)$	$12 \pm 4$	9.75	9.3	—	—	—
$(\pi^-, 4p \pi n)$	$6 \pm 2$	9.34	3.4	—	—	—
$(\pi^-, 5p \pi n)$	$1.5 \pm 0.2$	0.96	1.2	—	—	—

experimental data indicate predominant absorption of slow  $\pi^-$  by  $np$  pairs.

In Table II, we give the known experimental data on the measurement of the ratio of the probabilities of pion absorption by  $np$  and  $pp$  pairs.

It can be seen from Table II that the large experimental errors for  $R$  do not permit a definite value to be fixed for this quantity in calculations. It would be helpful to make a more accurate determination of  $R$  for light, medium, and heavy nuclei by the same method.

**Absorption of Negative Pions as a Method for Synthesizing New Isotopes.** It was shown in Ref. 40 that the process of disintegration of nuclei as a result of  $\pi^-$  absorption can be used as a method for synthesizing new isotopes. Neutron-deficient isotopes can be synthesized by using as targets the lightest stable isotopes of a given element, for example,  $^{96}\text{Ru}$ ,  $^{112}\text{Sn}$ ,  $^{154}\text{Sm}$ . The results of the calculations of Ref. 40 are plotted in the isotope chart in Fig. 15, in which the solid line is the boundary of known nuclei.<sup>93</sup> The hatched regions are the regions in which the probability  $W_{is}(A, Z)$  of production of the given isotope exceeds  $10^{-4}$  per absorbed pion. As can be seen in Fig. 14, when each of the light isotopes of the target nuclei Ru, Sn, and Sm are irradiated it is possible to have the production of several neutron-deficient isotopes of the nearest 6–8 elements. Bearing in mind that the calculation made in Ref. 40 strongly underestimates the yield of reactions with the maximal possible number of emitted particles  $x \geq 13$  (Figs. 13 and 14), one can hope to push the boundary of known nuclei forward by 1–2 units into the region of neutron deficiency.

If the heaviest isotopes of an element are used as a target, it follows from the calculations of Ref. 40 that already in the case of  $^{124}\text{Sn}$  and  $^{154}\text{Sm}$  targets one can pass the boundary of the known nuclei with neutron excess. The advance into the unknown region may be more appreciable if one uses the heavier stable nuclei  $^{176}\text{Yb}$ ,  $^{192}\text{Os}$ ,  $^{204}\text{Hg}$ ,  $^{238}\text{U}$ . In each case, even at a high

TABLE II. Experimental data on the ratio of the probabilities of absorption of a pion by  $np$  and  $pp$  pairs.

Nucleus	$R$	Reference	Nucleus	$R$	Reference
$^7\text{Li}$	$3.7 \pm 1.0$	[70]	N	$2.7 \pm 1.1$	[70]
$^9\text{Be}$	$3.3 \pm 0.9$	[70]	O	$3.8 \pm 1.0$	[70]
$^{10}\text{B}$	$2.3 \pm 0.8$	[70]	Al	$3.9 \pm 1.2$	[69]
$^{11}\text{B}$	$4.4 \pm 1.3$	[70]	Cu	$2.0 \pm 1.4$	[70]
C	$5.0 \pm 1.5$	[69]	Tm	$4.4 \pm 1.1$	[86]
	$2.5 \pm 1.0$	[70]	Pb	$4.7 \pm 4.7$	[70]
			Bi	$5.0 \pm 2.8$	[85]

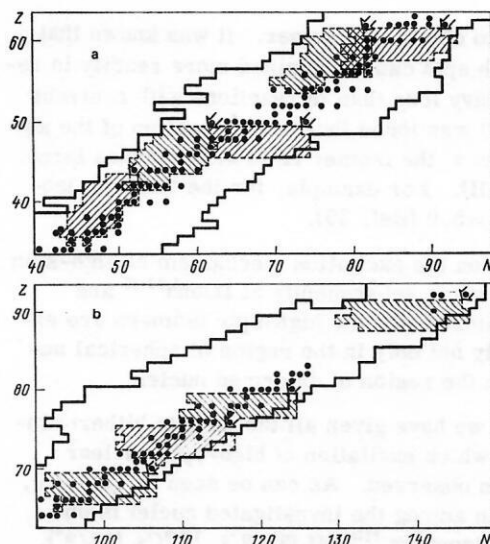


FIG. 15. Production of mesons after the absorption of slow  $\pi^-$  mesons by the nuclei  $^{96}\text{Ru}$ ,  $^{112}\text{Sn}$ ,  $^{124}\text{Sn}$ ,  $^{144}\text{Sm}$ ,  $^{154}\text{Sm}$  (a) and  $^{176}\text{Yb}$ ,  $^{192}\text{Os}$ ,  $^{204}\text{Hg}$ ,  $^{238}\text{U}$  (b) (Ref. 40). The black circles are stable isotopes and the arrows indicate the target nuclei.

level  $W_{is}(A, Z) \geq 10^{-4}$  one can expect the production of 4–7 unknown nuclei with neutron excess.

Unfortunately, it is difficult to compare the effectiveness of this method of synthesis with the usual methods of obtaining isotopes, since all the calculations are normalized to one absorbed pion. However, one can roughly estimate the possibilities of the method by considering the beam parameters of operating accelerators. For example, for the meson factories one can achieve a total rate of stoppings of about  $10^8$ – $10^9$  negative pions per second.<sup>95</sup> In this case, the total rate of production of an isotope in the hatched region in Fig. 15 exceeds  $10^4$  nuclei/sec. It is to be hoped that these high rates will make it possible to penetrate into the region where  $W_{is} < 10^{-4}$ .

Thus, disintegration of nuclei resulting from the absorption of negative pions can also be used to obtain and investigate properties of nuclei with both neutron deficit and neutron excess.

#### 4. EXCITATION OF HIGH-SPIN STATES RESULTING FROM THE ABSORPTION OF NEGATIVE PIONS BY NUCLEI

Until the appearance of the first experimental papers of Refs. 34 and 35, no theoretical calculations had been made of the possibility of excitation by pions of states with high spins  $(10-20)\hbar$ . In the experimental investigation of the process of production of thallium isotopes in the capture reaction of negative pions by lead nuclei it was found that for the isotopes  $^{196}\text{Tl}$  and  $^{198}\text{Tl}$  isomer states with spin  $7\hbar$  are populated with high probability.<sup>35</sup>

The intensity of production of metastable states can be characterized by the isomer ratio. The isomer ratio  $\xi = \sigma_m / \sigma_g$  characterizes the ratio of the cross sections for the production of the isotope in the isomer state and in the ground state. This ratio depends strongly on both the energy and spin of the level and also on the type of



reaction used to obtain the isomer. It was known that states with high spin can be obtained more readily in reactions with heavy ions than in reactions with neutrons and protons. It was found that in the reaction of the absorption of slow  $\pi^-$  the isomer ratio also reaches large values (Table III). For example, for the thallium isotopes  $\xi = \sigma_m/\sigma_g = 5.0$  (Ref. 35).

Experiments on the excitation mechanism of high-spin nuclear states made subsequently at Dubna<sup>80-86</sup> and SIN<sup>64,66,88</sup> confirmed that the high-spin isomers are excited effectively not only in the region of spherical nuclei but also in the region of deformed nuclei.

In Table IV, we have given all the targets hitherto investigated for which excitation of high-spin nuclear states has been observed. As can be seen in Table IV, the highest spin among the investigated nuclei is observed for the isomers  $^{177m}\text{Hf}$  (37/2<sup>-</sup>),  $^{135m}\text{Cs}$  (19/2<sup>-</sup>),  $^{150m}\text{Tb}$  (9<sup>+</sup>),  $^{204m}\text{Pb}$  (9<sup>-</sup>),  $^{152m}\text{Eu}$  (8<sup>-</sup>),  $^{198m}\text{Au}$  (12<sup>-</sup>). In Fig. 16, we give as an example part of the  $\gamma$ -ray spectrum of the lead isotopes  $^{197m}\text{Pb}$ ,  $^{199m}\text{Pb}$ , and  $^{201m}\text{Pb}$  with spins (13/2) $\hbar$ , and also  $^{202m}\text{Pb}$  and  $^{204m}\text{Pb}$  with spins 9 $\hbar$ , which are produced as a result of pion capture by  $^{209}\text{Bi}$  nuclei. It can be seen that all the strong  $\gamma$  lines in the spectrum belong to high-spin lead isomers.

These experimental facts evoked great interest. It was not clear how such large angular momenta of the residual nucleus could arise if the orbital angular momentum  $l$  of the pion in the orbit of the mesic atom from which it is captured is low ( $l \leq 3\hbar$ ). In such a case, since the spin of the product nucleus greatly exceeds the maximal possible total value of the spin of the initial nucleus and the orbital angular momentum introduced by the pion, it was necessary to expect an extremely low probability of excitation of high-spin states. The explanation of the excitation of high-spin isomer states, which indicates the formation after the pion absorption of residual nuclei with large angular momentum  $M$ , was first given in Ref. 96, and then essentially similar explanations were given in Refs. 44, 90, and 97. It was shown in these papers that fast nucleons, the products of two-nucleon absorption of the pion emitted from the surface layer of the nucleus during the stage of the intranuclear cascade, are responsible for the large angular momentum.

If one ignores the angular momentum introduced by the capture of the pion from the orbit of the mesic atom and the spins of the nucleus and the particles, then from the law of conservation of angular momentum

$$M \approx - \sum_i m_i, \quad (13)$$

where  $M$  is the angular momentum of the residual nucleus, and  $m_i$  is the angular momentum introduced by the cascade particle.

In Fig. 17, the distribution of the residual nuclei with respect to the absolute magnitude of the angular momentum<sup>58</sup> is shown. In the case of heavy target nuclei, there are formed after the intranuclear cascade residual nuclei whose angular momentum may reach (15–17) $\hbar$ . Thus, with allowance for the spins and the orbital angular momentum introduced by the pion, the angular

TABLE III. Experimental values of  $\sigma_m/\sigma_g$ .

Reaction	Nucleide	$\sigma_m/\sigma_g$	Ground state		Isomer state		$\sigma_m/\sigma_g$ from other reactions
			$I\pi$	$E_\gamma$ , keV	$I\pi$	$E_\gamma$ , keV	
$^{208}\text{Pb}(\pi^-, 10n)$	$^{198}\text{Tl}$ 81	5.0	2 <sup>-</sup>	675.8	7 <sup>+</sup>	282.8	—
$^{200}\text{Hg}(\pi^-, 1-4n)$	$^{200}\text{Au}$ 79	$0.16 \pm 0.05$	1 <sup>-</sup>	579.3	12 <sup>-</sup>	1225.5	0.17 (p, pn)
$^{200}\text{Hg}(\pi^-, 2-6n)$	$^{198}\text{Au}$ 79	$0.20 \pm 0.05$	2 <sup>-</sup>	411.8	12 <sup>-</sup>	214.9	—
$^{200}\text{Hg}(\pi^-, 4-8n)$	$^{198}\text{Au}$ 79	$0.35 \pm 0.07$	2 <sup>-</sup>	355.7	12 <sup>-</sup>	117.7	0.36 (11B, $\alpha$ 3n)
$^{194}\text{Pt}(\pi^-, 4-8n)$	$^{190}\text{Ir}$ 77	$0.25 \pm 0.05$	4 <sup>+</sup>	518.5	11 <sup>-</sup>	361.2	0.025 ( $\alpha$ , 2n)
$^{168}\text{Er}(\pi^-, 4n)$	$^{162}\text{Ho}$ 67	$1.3 \pm 0.3$	1 <sup>+</sup>	1319.6	6 <sup>-</sup>	1220.0	—
$^{118}\text{Sn}(\pi^-, 6-8n)$	$^{118}\text{In}$ 49	$3.0 \pm 0.5$	1 <sup>+</sup>	617.1	4 <sup>+</sup>	155.5	—
$^{118}\text{Sn}(\pi^-, 8-10n)$	$^{118}\text{In}$ 49	$0.25 \pm 0.50$	2 <sup>+</sup>	657.5	7 <sup>+</sup>	884.7	—
$^{118}\text{Sn}(\pi^-, 10-12n)$	$^{108}\text{In}$ 49	0.2	3 <sup>+</sup>	633.2	5, 6 <sup>+</sup>	876.0	—

momenta of the residual nuclei can exceed 20 $\hbar$ . Such high values of the angular momentum of the residual nuclei are comparable with the  $M$  values obtained in heavy-ion reactions. But whereas in the latter the angular momentum is introduced into the nucleus by the incident particle, in pion reactions the additional angular momentum is produced by the emission of fast particles from the surface layer of the nucleus.

The heavier the nucleus, the higher the spin which the residual nucleus can populate, since the  $M$  distribution for light nuclei is shifted to the region of small  $M$ . In Fig. 18, we plot the mean angular momentum of the residual nuclei as a function of the atomic number of the target nucleus in accordance with the law  $\bar{M} \approx 0.92A^{1/3}$ , which is a direct reflection of the surface nature of the  $\pi^-$  absorption by the nucleus.

The phenomenon of excitation of high-spin states must be observed not only in the case of  $\pi^-$  absorption by nuclei but also in all processes accompanied by the emission from the nucleus of fast particles, for example, in reactions in which nuclei are disintegrated by particles of medium energy. However, the total distribution of the residual nuclei with respect to the angular momentum is not a sufficiently sensitive characteristic whose investigation could give information about the mechanism of absorption of different particles by nuclei. The validity of this assertion was demonstrated in Ref. 98 by comparing two reactions—the absorption of slow  $\pi^-$  mesons and of  $\gamma$  rays with energy  $E_\gamma = m_\pi$ . It is well known that the mechanism of absorption of  $\gamma$  rays of such energy is also a quasideuteron mechanism, but in contrast to the  $\pi^-$  mesons the absorption takes place uniformly over the complete volume of the nucleus. The calculations of Ref. 98 showed that the distributions of the residual nuclei with respect to the angular momentum in the two reactions are similar (Fig. 19).

Theoretical and experimental investigations<sup>44</sup> of proton-nucleus reactions at energy  $E_p = m_\pi/2$  showed that not only the values of the angular momenta of the residual nuclei but also the isomer ratios for some states are close to the observed values of  $\sigma_m/\sigma_g$  in reactions in

TABLE IV. Observed high-spin states of isomers produced in meson absorption reactions.

Target nucleus	$J_i$	$ZA (\pi^-, \pi n) (Z-1)^A-x$	$ZA (\pi^-, p \pi n) (Z-2)^A-x-1$	$ZA (\pi^-, 2p \pi n) (Z-3)^A-x-2$
		$J_f, T_{1/2}$	$J_f, T_{1/2}$	$J_f, T_{1/2}$
$^{209}_{83}\text{Bi}$	9/2-	$^{199}\text{mPb}$ (13/2 <sup>+</sup> ; 12 min) $^{202}\text{mPb}$ (9 <sup>-</sup> ; 3.62 h)	$^{196}\text{mTl}$ (7 <sup>+</sup> , 1.4 h) $^{198}\text{mTl}$ (7 <sup>+</sup> , 1.87 h)	—
$^{208}_{82}\text{Pb}$	0 <sup>+</sup>	$^{196}\text{mTl}$ (7 <sup>+</sup> ; 1.4 h) $^{198}\text{mTl}$ (7 <sup>+</sup> ; 1.87 h)	$^{193}\text{mHg}$ (13/2 <sup>+</sup> ; 11.1 h) $^{195}\text{mHg}$ (13/2 <sup>+</sup> ; 40 h)	—
$^{203, 205}_{81}\text{Tl}$	1/2 <sup>+</sup>	$^{197}\text{mHg}$ (13/2 <sup>+</sup> ; 23.8 h) $^{199}\text{mHg}$ (13/2 <sup>+</sup> ; 42.6 min)	$^{196}\text{mAu}$ (12 <sup>-</sup> ; 9.7 h) $^{198}\text{mAu}$ (12 <sup>-</sup> ; 2.3 days) $^{200}\text{Au}$ (12 <sup>-</sup> ; 18.7 h)	—
$^{198-204}_{80}\text{Hg}$	0 <sup>+</sup> 5/2-	$^{196}\text{mAu}$ (12 <sup>-</sup> ; 9.7 h) $^{200}\text{mAu}$ (12 <sup>-</sup> ; 18.7 h)	$^{197}\text{mPt}$ (13/2 <sup>+</sup> ; 81 min) $^{195}\text{mPt}$ (13/2 <sup>+</sup> ; 4.02 days)	—
$^{197}_{79}\text{Au}$	3/2 <sup>+</sup>	$^{197}\text{mPt}$ (13/2 <sup>+</sup> ; 81 min) $^{195}\text{mPt}$ (13/2 <sup>+</sup> ; 4.02 days)	$^{190}\text{mIr}$ (11 <sup>-</sup> , 3.2 h)	—
$^{194-198}_{78}\text{Pt}$	0 <sup>+</sup> 1/2-	$^{190}\text{mIr}$ (11 <sup>-</sup> ; 3.2 h)	—	—
$^{181}_{73}\text{Ta}$	7/2 <sup>+</sup>	$^{177}\text{m}_2\text{Hf}$ (37/2 <sup>-</sup> ; 51.4 min)	$^{172}\text{Lu}$ (4 <sup>-</sup> ; 6.7 days)	—
$^{178}_{68}\text{Tm}$	1/2-	—	$^{156}\text{Ho}$ (5 <sup>+</sup> ; 55 min) $^{158}\text{Ho}$ (5 <sup>+</sup> ; 11 min) $^{160}\text{Ho}$ (5 <sup>+</sup> ; 26 min) $^{162}\text{m}_2\text{Ho}$ (6 <sup>-</sup> ; 68 min)	—
$^{170-172}_{68}\text{Er}$	(0 <sup>+</sup> ; 7/2 <sup>+</sup> )	$^{156}\text{Ho}$ (5 <sup>+</sup> ; 55 min) $^{158}\text{Ho}$ (5 <sup>+</sup> ; 11 min) $^{160}\text{Ho}$ (5 <sup>+</sup> ; 26 min) $^{162}\text{m}_2\text{Ho}$ (6 <sup>-</sup> ; 68 min)	—	—
$^{165}_{67}\text{Ho}$	7/2-	—	$^{154}\text{m}_2\text{Tb}$ (6 <sup>-</sup> ; 22.6 h)	—
$^{164}_{66}\text{Dy}$	(0 <sup>+</sup> ; 5/2-)	$^{150}\text{mTb}$ (9 <sup>+</sup> ; 5.8 min)	—	$^{152}\text{m}_2\text{Eu}$ (8 <sup>-</sup> ; 96 min)
$^{159}_{65}\text{Tb}$	3/2 <sup>+</sup>	—	$^{152}\text{m}_2\text{Eu}$ (8 <sup>-</sup> ; 96 min)	—
$^{160}_{64}\text{Gd}$	(0 <sup>+</sup> ; 3/2-)	$^{152}\text{m}_2\text{Eu}$ (8 <sup>-</sup> ; 96 min)	—	$^{148}\text{mPm}$ (6 <sup>-</sup> ; 41.3 days)
$^{153}_{63}\text{Eu}$	5/2 <sup>+</sup>	$^{141}\text{mSm}$ (11/2 <sup>-</sup> ; 22.6 min)	—	$^{139}\text{mNd}$ (11/2 <sup>-</sup> ; 5.5 h)
$^{154-156}_{62}\text{Sm}$	(0 <sup>+</sup> ; 7/2-)	$^{140}\text{mPm}$ (8 <sup>-</sup> ; 5.8 min)	$^{139}\text{mNd}$ (11/2 <sup>-</sup> ; 5.5 h)	$^{138}\text{mPr}$ (1 <sup>-</sup> ; 2.1 h)
$^{150-152}_{60}\text{Nd}$	(0 <sup>+</sup> ; 7/2-)	$^{138}\text{mPr}$ (7 <sup>-</sup> ; 2.1 h)	—	—
$^{141}_{59}\text{Pr}$	5/2 <sup>+</sup>	$^{137}\text{mCe}$ (11/2 <sup>-</sup> ; 34.4 h)	—	$^{135}\text{mBa}$ (11/2 <sup>-</sup> ; 28.7 h)
$^{142}_{58}\text{Ce}$	0 <sup>+</sup>	—	$^{137}\text{mBa}$ (11/2 <sup>-</sup> ; 2.55 min)	—
$^{138}_{57}\text{La}$	7/2 <sup>+</sup>	$^{133}\text{mBa}$ (11/2 <sup>-</sup> ; 38.9 h) $^{137}\text{mBa}$ (11/2 <sup>-</sup> ; 2.55 min)	$^{134}\text{mCs}$ (8 <sup>-</sup> ; 2.9 h) $^{135}\text{mCs}$ (19/2 <sup>-</sup> ; 53 min)	—
$^{138-139}_{56}\text{Ba}$	(0 <sup>+</sup> ; 3/2 <sup>+</sup> )	$^{135}\text{mCs}$ (19/2 <sup>-</sup> ; 53 min)	—	—
$^{133}_{55}\text{Cs}$	7/2 <sup>+</sup>	—	$^{130}\text{I}$ (5 <sup>-</sup> ; 12.4 h)	—
$^{127}_{53}\text{I}$	5/2 <sup>+</sup>	—	$^{116}\text{mSb}$ (8 <sup>-</sup> ; 60 min) $^{118}\text{mSb}$ (8 <sup>-</sup> ; 5.0 h) $^{120}\text{mSb}$ (8 <sup>-</sup> ; 5.76 days)	—
$^{121, 123}_{51}\text{Sb}$	5/2 <sup>+</sup> 7/2 <sup>+</sup>	—	$^{110}\text{mIn}$ (7 <sup>+</sup> ; 4.9 h) $^{112}\text{mIn}$ (4 <sup>+</sup> ; 20.9 min) $^{114}\text{mIn}$ (5 <sup>+</sup> ; 49.5 days)	$^{111}\text{mCd}$ (11/2 <sup>-</sup> ; 48.6 min)

Target nucleus	$J_i$	$Z A (\pi^-, xn) (Z-1)^{A-x}$	$Z A (\pi^-, pxn) (Z-2)^{A-x-1}$	$Z A (\pi^-, 2pxn) (Z-3)^{A-x-2}$
		$J_f, T_{1/2}$	$J_f, T_{1/2}$	$J_f, T_{1/2}$
$^{112-122}_{50}\text{Sn}$	$0^+ - 9/2^+$	$^{108\text{m}}\text{In} (5, 6^+; 58 \text{ min})$ $^{110\text{m}}\text{In} (7^+; 4.9 \text{ h})$	$^{111\text{m}}\text{Cd} (11/2^-; 48.6 \text{ min})$	—
$^{113}_{51}\text{In}$	$9/2^+$	$^{111\text{m}}\text{Cd} (11/2^-; 48.6 \text{ min})$	—	—
$^{106-116}_{48}\text{Cd}$	$0^+; 1/2^+$	$^{106\text{m}}\text{Ag} (6^+; 8.3 \text{ days})$	$^{109\text{m}}\text{Pd} (11/2^-; 4.69 \text{ min})$ $^{111\text{m}}\text{Pd} (11/2^-; 5.54 \text{ min})$	—
$^{107}_{47}\text{Ag}$	$1/2^-$	—	$^{106\text{m}}\text{Rh} (5, 6^+; 2.2 \text{ h})$	$^{47}\text{Ag} (\pi^-, 3pxn) ^{44}\text{Tc} (6, 7^+; 4.9 \text{ h})$ $^{47}\text{Ag} (\pi^-, 4pxn) ^{43}\text{Mo} (21/2^+; 6.8 \text{ h})$
$^{101-110}_{46}\text{Pd}$	$0^+ - 5/2^+$	$^{106\text{m}}\text{Rh} (5, 6^+; 2.2 \text{ h})$	—	$^{96\text{m}}\text{Tc} (4^+; 52 \text{ min})$

which slow nucleons are absorbed (Table V).

It is now known<sup>40, 87</sup> that the isomer ratio depends on a number of characteristics of the reaction, namely, the spins of the isomer state and the ground state, the number of emitted particles, and the total number of particles which participate in the formation of these states. Therefore, from the single measurement made in Ref. 44 it is difficult to determine the form of this dependence, and it is even harder to extract information about the distribution of the residual nuclei with respect to the angular momentum.

Already the first experiments<sup>80-84</sup> that studied the isomer ratio showed that the isomer ratio for the excitation of metastable states with equal spins increases with increasing number of emitted nucleons (see Table III). To elucidate how the isomer ratio depends on the number of emitted particles, it is necessary to investigate  $\sigma_m/\sigma_g$  for a sufficiently large fixed value of the spin for different values of  $x$  in a wide range, for example, from 2 to 14.

In Refs. 40 and 96, the dependence of the mean angular momentum  $M$  on the number  $x$  of emitted particles was determined. It is easy to show that not all values of  $x$  are equally effective for populating high-spin states. Let us consider as an example the  $(\pi^-, xn)$  reaction.

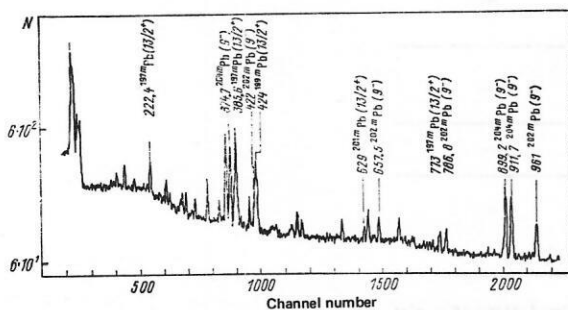


FIG. 16. Section of the  $\gamma$ -ray spectrum of lead isotopes produced by the capture of slow  $\pi^-$  mesons by bismuth nuclei.

The case of maximal  $x$ , when all the cascade particles are absorbed by the nucleus and then only evaporation neutrons are emitted from it isotropically, corresponds to small values of  $M$  [see (13)]. The other limiting case  $x=2$ , when after the absorption by an  $np$  pair two neutrons are emitted in opposite directions, also gives a small value of the angular momentum of the residual nucleus. And, obviously, the maximal angular momentum is realized when after absorption in the surface layer one fast neutron is emitted without undergoing collisions, and the other is absorbed in the nucleus. Then from a compound nucleus with excitation energy  $E^* \approx m_\pi/2$  there are emitted on the average 5-6 evaporation neutrons, i. e., in the case of surface absorption the dependence of the mean angular momentum  $\overline{M}(x)$  will have a maximum at  $x=6-7$  (Fig. 20). As can be seen in Fig. 20, in the case of volume absorption of  $\gamma$  rays the dependence  $\overline{M}(x)$  has a different form.

Usually, in experiments it is not the angular momenta of the residual nuclei that are measured but rather the isomer ratios.<sup>80-84</sup> However, the calculated dependence  $\overline{M}(x)$  can be compared with the experimental dependence  $\xi(x)$  for the excitation of isomer states with sufficiently

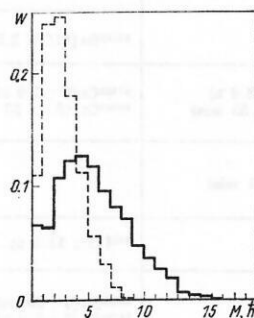


FIG. 17. Distribution of residual nuclei produced after absorption of  $\pi^-$  mesons by  $^{31}\text{P}$  nuclei (broken line) and  $^{208}\text{Pb}$  nuclei (solid line) with respect to the angular momentum  $M$  (Ref. 58). The distributions are normalized to one pion absorption.



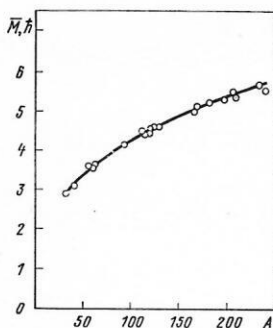


FIG. 18. Dependence of the mean angular momentum  $\bar{M}$  on the atomic number  $A$  of the target nucleus. The open circles are the calculation of Ref. 58 and the continuous curve is the approximation  $\bar{M} = 0.92 A^{1/3}$ .

large fixed value of the spin. It should also be noted that the mean angular momentum  $\bar{M}(x)$  of the residual nucleus is calculated without allowance for the orbital angular momentum of the pion  $l_r$ , the spin of the target nucleus  $I_{in}$ , and also the angular momenta introduced by the evaporation particles  $\sum m_i^{evap}$ . Although the values of  $l_r$ ,  $I_{in}$ , and  $\sum m_i^{evap}$  are less than the angular momentum carried away by the cascade particles, they can distort the form of the dependence  $\bar{M}(x)$ . For this reason, one should choose target nuclei with spins  $I_{in} = 0$  in a comparison.

The experimental investigations showed that the probability of excitation of high-spin isomers does indeed depend on the number of emitted neutrons in approximately the manner predicted by theory. In Ref. 81, a study is made of the dependence of the probability of production of the high-spin isomers  $^{108m}\text{In}(7^+)$  and  $^{110m}\text{In}(7^+)$  on the number of emitted neutrons in the case of  $\pi^-$  absorption by the tin nuclei  $^{112}\text{Sn}$ ,  $^{114}\text{Sn}$ ,  $^{118}\text{Sn}$ ,  $^{120}\text{Sn}$ ,  $^{122}\text{Sn}$ , and  $^{124}\text{Sn}$  with spins  $I_{in} = 0$ . The values of the isomer ratios  $\sigma_m/\sigma_g$  (in relative units) as functions of the number  $x$  of emitted neutrons are shown in Fig. 21. It can clearly be seen that the isomer ratio increases as the neutron multiplicity increases from 2 to 6, and then falls with further increase in  $x$ . The dependence has a maximum at  $x = 6-7$ , which corresponds to an excitation energy  $m_\pi/2 \approx 70$  MeV of the nucleus. These data are a direct proof of the surface nature of the absorption of slow pions by a pair of nucleons.

Unfortunately, there are as yet no calculations of the

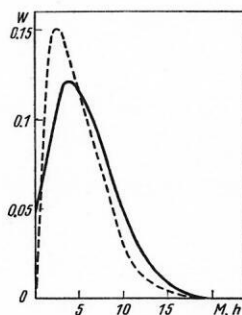


FIG. 19. Distribution of residual nuclei formed after absorption of slow  $\pi^-$  mesons (continuous curve) and  $\gamma$  rays with  $E_\gamma = 140$  MeV (broken curve) by  $^{208}\text{Pb}$  nuclei with respect to the angular momentum  $M$ .

TABLE V. Isomer ratios for the isotopes  $^{174}\text{Lu}$  and  $^{177}\text{Lu}$ .

Isotope	Spin of ground state	Spin of isomer state	Protons $E_p = 100$ MeV	Protons $E_p = 500$ MeV	Slow $\pi^-$ mesons
$^{174}\text{Lu}$	$1^-$	$6^-$	$0.65 \pm 0.08$	$0.65 \pm 0.07$	$0.69 \pm 0.07$
$^{177}\text{Lu}$	$7/2^+$	$23/2^-$	$0.19 \pm 0.12$	$0.088 \pm 0.030$	$0.15 \pm 0.04$

isomer ratios for high-spin states of the residual nuclei produced by the absorption of pions by nuclei. It would be interesting to attempt to describe the high values of the isomer ratios in the models of Refs. 40 and 44.

It is evident that Refs. 40 and 44 correctly indicate that the main source of the high angular momentum of the residual nuclei in the case of pion absorption is the fast nucleons. However, it would also be very attractive to investigate other mechanisms of formation of large angular momentum of residual nuclei. One such mechanism is the fluctuation mechanism, in which a large angular momentum of the residual nucleus can be produced by the random addition of the angular momenta carried away by the evaporation particles. A possible indication of such a mechanism can be seen in the data of Ref. 88, in which it was found that when  $\pi^-$  mesons are absorbed by the  $^{181}\text{Ta}$  nucleus up to 13 neutrons are emitted and at the same time states with spin  $16\hbar$  can be excited with low probability ( $\sim 10^{-3}$  per 1 pion).

Thus, the method of studying the mechanism of absorption of slow  $\pi^-$  by nuclei by means of the excitation and investigation of high-spin states is very topical and not all possibilities have been exhausted. With regard to other nuclear reactions initiated by particles of medium energy, for them systematic investigations of the angular momenta of the residual nuclei (and accordingly the isomer ratios) are not available, so that there is great scope for work in this direction.

## 5. MOMENTUM OF THE RESIDUAL NUCLEUS

It follows from what we have said above that the investigation of characteristics of the residual nucleus such as the angular momentum has yielded valuable information about the mechanism of pion absorption by nuclei. A further important characteristic of the residual nucleus is its momentum  $P$ . In the region of light nuclei, the recoil momentum is usually measured with a view to investigating the momentum distribution of the many-nucleon association that absorbs the pion in the nucleus. In the case of a light nucleus, from which the

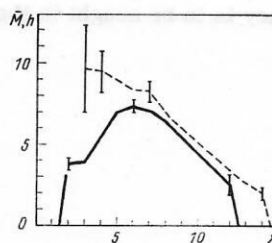


FIG. 20. Dependence of the mean angular momentum  $\bar{M}$  on the number of emitted particles. The solid curve is the calculation of Ref. 98 for the reaction  $^{208}\text{Pb}(\pi^-, xn)$ , the broken curve for the reaction  $^{208}\text{Pb}(\gamma, xn)$ ; the statistical errors of the calculation are indicated.

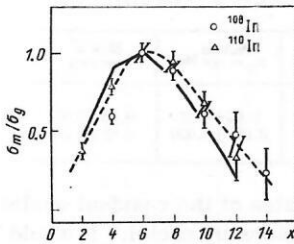


FIG. 21. Dependence of the isomer ratio  $\sigma_m/\sigma_g$  on the number of emitted particles in the reaction  $\text{Sn}(\pi^-, xn)\text{In}$ . The solid curve is the calculation of Ref. 58 and the broken curve the experiment of Ref. 81.

absorption products are emitted without interaction with intranuclear nucleons, it is indeed possible to relate the recoil momentum of the nucleus with sufficient confidence to the momentum of the association.

For the simplest  $(\pi^-, 2n)$  reaction, the momentum of the nucleus can be extracted from an analysis of a kinematically complete experiment with measurement of the energies of the two neutrons.<sup>74-76</sup> A measurement of the recoil momentum by means of the Doppler effect can in principle be used for a wider range of residual nuclei (Refs. 38, 92, and 99-101).

In the models of Refs. 39, 40, and 44, the momentum of the nucleus produced after the termination of the intranuclear cascade is determined by the simple relation

$$\vec{P} \approx - \sum_i \vec{p}_i, \quad (14)$$

where  $\vec{p}_i$  is the momentum of the cascade particle. The calculations of Ref. 58 showed that the mean momentum of the residual nucleus is virtually independent of the mass number of the target nucleus and equal to  $\bar{P} \approx 220$  MeV/c. In contrast to the angular momentum, the distributions of the residual nuclei with respect to the momentum  $P$  also depend weakly on the target nucleus (Fig. 22).

In Fig. 23, we compare with the experiments the calculated dependence of the mean momentum  $\bar{P}$  of the nucleus on the number of nucleons  $\Delta A$  carried away from the target after absorption in it of a pion. At small  $\Delta A \ll 4$ , the momentum  $\bar{P}$  increases with increasing  $\Delta A$ , and then depends weakly on  $\Delta A$ . At small values of  $\Delta A$ , there is reasonable agreement with the experimental values of  $\bar{P}$ , but for  $\Delta A \geq 4$  the experiment lies much higher than the theory.

The reason for this discrepancy is to be sought in the

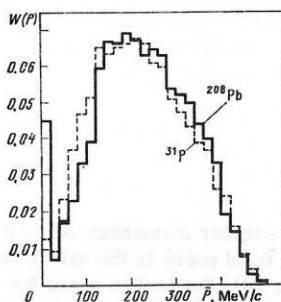


FIG. 22. Momentum distribution of the residual nuclei produced after absorption of  $\pi^-$  mesons by the nuclei  $^{31}\text{P}$  and  $^{208}\text{Pb}$ .

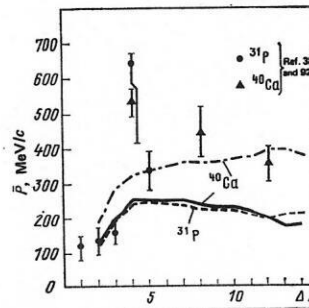


FIG. 23. Dependence of the mean momentum  $\bar{P}$  of the residual nucleus on the number of nucleons  $\Delta A$  emitted by the target nucleus. The broken curve is a calculation for  $^{40}\text{Ca}$  with allowance for pre-equilibrium and evaporation particles.<sup>58</sup>

change in the momentum of the residual nucleus due to the emission from it of pre-equilibrium and evaporation particles. Allowance for the contribution of the momenta of these particles to the momentum of the residual nucleus as a whole improves the agreement with the experiment (see Fig. 23), but some experimental points are above the theoretical curve. It is possible that the experimental data are somewhat overestimated by the need to specify the form of the momentum distribution of the recoil nuclei when  $\bar{P}$  is deduced.

The experiments initiated in Refs. 38, 92, and 99-101 require a further development, both as regards their method and in the measurement of the other characteristics of the nuclear reaction. In particular, using the Doppler effect to measure the mean momentum of the nucleus for states with different fixed values of the spin  $M$ , one could determine the correlation between the mean value of  $\bar{P}$  and the angular momentum  $M$  of the nucleus.

## 6. FISSION OF NUCLEI AFTER ABSORPTION OF SLOW $\pi^-$ MESONS. SEARCH FOR DELAYED FISSION

**Fission.** Highly excited compound states can shed their excitation not only by emitting particles but also by fission. Moreover, in the case of absorption of stopped  $\pi^-$  mesons one can have fission of strongly fissioning nuclei with mass  $A > 230$  and weakly fissioning nuclei with  $A < 200$ , since the excitation energy of the nucleus may reach 140 MeV (see Fig. 8). Indeed, in

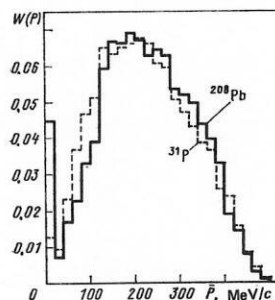


FIG. 24. Yield of actinium isotopes per absorbed pion in the reaction  $^{232}\text{Th}(\pi^-, xn)^{232}\text{Ac}$ . The solid line is the calculation of Ref. 58 without allowance for fission, and the broken line is with allowance for it. The experimental data are taken from Ref. 108.

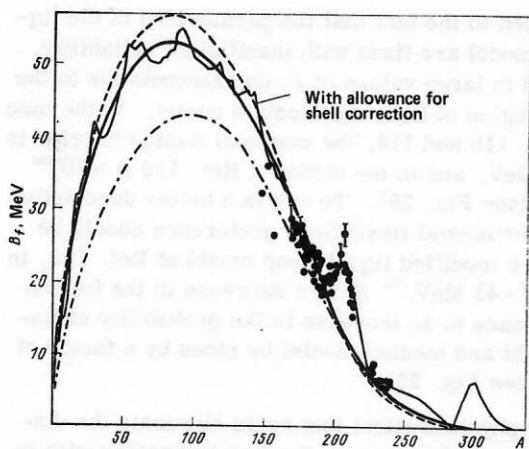


FIG. 25. Heights of the fission barrier of nuclei along the  $\beta$ -stability line. The solid curve is the calculation in accordance with the liquid-drop model<sup>115</sup> with and without allowance for the shell correction; the broken curve is the calculation in accordance with the liquid-drop model with the parameters of Pauli and Ledergerber<sup>119</sup>; the chain curve is the calculation in accordance with the modified liquid-drop model of Ref. 120 without allowance for shell corrections.

the experiments of Refs. 102–107 fission by stopped pions of both heavy and medium nuclei was observed.

In the region of the strongly fissioning nuclei  $^{235}\text{U}$  and  $^{232}\text{Th}$ , whose fission probability is several tens of percent, the competition between the processes of particle evaporation and fission influences the various characteristics of the reaction. One such characteristic is the isotope yield. As was shown in Ref. 40, fission must lead to a narrower distribution of the isotope yield. Because the fissility of a nucleus increases strongly with decreasing number of neutrons in it,<sup>56</sup> the fraction of neutron-deficient nuclei that avoid fission decreases sharply (Fig. 24). Therefore, the growth in Fig. 10 of the width of the isotope-yield curves with a further increase in the mass number must cease and the width must decrease in the region of Th and U. Unfortunately, there are no measurements of the isotope-yield curve for strongly fissioning targets. The unique experimental point<sup>108</sup> on the isotope-yield curve from a thorium target agrees with the calculations and confirms the general tendency for a decrease in the yield of neutron-deficient isotopes. Thus, fission strongly restricts the possibility of obtaining neutron-deficient isotopes from uranium and transuranium targets.

The fission probability (fissility) of nuclei by slow  $\pi^-$  mesons decreases with decreasing atomic number of the target nucleus (Fig. 25). The fissility is analyzed as a function of  $A$  in Refs. 40, 59, and 109. It is shown in these papers that the experimental fissilities of nuclei by pions can be described in the framework of the two-nucleon absorption mechanism by using the methods of calculating the fission of nuclei by protons of medium energy<sup>40</sup> or the fission barriers  $B_f$  extracted from experiments with low-energy particles.<sup>59,109</sup> In Refs. 59 and 109, it was shown that the calculated fissilities of nuclei by pions are very sensitive to the ratio  $a_f/a$  of the density parameters of the levels of the nucleus at the saddle point and in an ordinary excited state. To

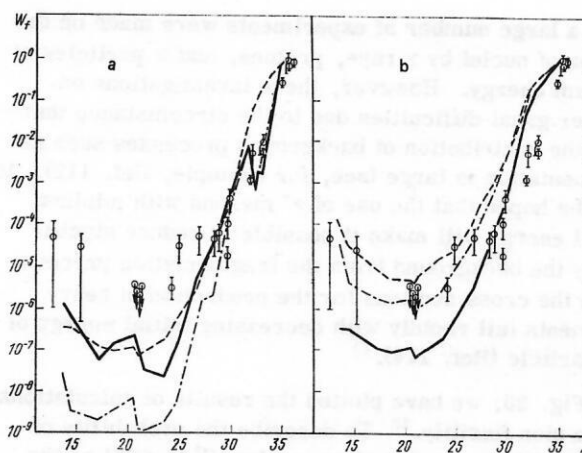


FIG. 26. Fission probability  $W_f$  as a function of  $Z^2/A$  of the target nucleus. a) The continuous line is the calculation with the barriers of Ref. 115 for  $a_f/a=1.1$ ; the broken curve is the calculation for the same parameters without allowance for shell effects; the chain curve is the calculation for  $a_f/a=1.2$  with allowance for pre-equilibrium emission of the particles. b) The solid line is the calculation with the barriers of Ref. 115 for  $a_f/a=1.1$  without allowance for shell effects; the broken curve is the calculation with the same set of parameters but with the Krappe-Nix barriers<sup>120</sup>; the chain curve is a calculation with allowance for "thermal" effects. The experimental data are taken from Refs. 106 and 107.

describe the experimental data, the authors of Ref. 59 used the ratio  $a_f/a=1.2$ , and in Ref. 109 the ratio  $a_f/a=1.1$  was obtained. It should be noted that similar values of  $a_f/a$  are obtained in experiments on the fission of highly excited compound nuclei produced in reactions with low-energy  $\alpha$  particles.<sup>110,111</sup> These conclusions agree with the results of Ref. 112 in a theoretical analysis of the fissility of nuclei by protons of medium energy, in which a strong sensitivity of the fissility to the ratio  $a_f/a$  is also noted. The value  $a_f/a=1.05$  found in Ref. 112 for 150-MeV protons agrees better with the results obtained in Ref. 109. The value  $a_f/a=1.2$  in Ref. 59 appears to be overestimated, which can be explained by the use in Ref. 59 of a very simplified model to describe the stage of pion absorption by the nucleus.

Another problem is currently more topical: How can new information about the properties of highly excited nuclei be extracted by analyzing experiments in which the fissility of nuclei is measured? This is inseparably related to the answer of the question relating to the as yet obscure details of the absorption process that can influence the fissility.

Above all, from an analysis of the fissility of nuclei by pions of medium energy one can obtain information about the height of the fission barriers in the uninvestigated region of medium and light nuclei. Modern models of fission predict that the height of the fission barrier must initially increase with a decrease in  $A$ , reaching a maximal value  $B_f^{\text{max}}$  at  $A \approx 80-100$ , and then decrease in the region of light nuclei (Fig. 25). On the basis of this fact, the paper of Ref. 113 predicts a decrease in the fissility to a minimal value at  $A \approx 80-100$ , and then again an increase in the region of light nuclei.

To detect this increase in the fissility of medium nu-



clei, a large number of experiments were made on the fission of nuclei by  $\gamma$  rays, protons, and  $\alpha$  particles of medium energy. However, these investigations encounter great difficulties due to the circumstance that here the contribution of background processes such as fragmentation is large (see, for example, Ref. 112). It is to be hoped that the use of  $\pi^-$  mesons with minimal initial energy will make it possible to reduce significantly the background from the fragmentation process, since the cross sections for the production of heavy fragments fall rapidly with decreasing initial energy of the particle (Ref. 114).<sup>4)</sup>

In Fig. 26, we have plotted the results of calculations of the pion fissility.<sup>58</sup> To describe the probability of fission of heavy and medium nuclei ( $Z^2/A \leq 27$ ) on the basis of the widely used liquid-drop model,<sup>115</sup> it is necessary to take the ratio  $a_f/a = 1.1$ , as in Ref. 109. In the region of the doubly magic nucleus  $^{208}\text{Pb}$ , the discrepancy with experiment is appreciable, which indicates a need for a more rigorous allowance for shell effects in the level density of the nucleus. A convenient approximation for the level-density parameter is obtained in Ref. 116:

$$a(E^*, A, Z) = \tilde{a} \{1 + [1 - \exp(-0.061E^*)] \Delta M/E^*\}, \quad (15)$$

where  $\Delta M$  is the shell correction to the mass of the nucleus, and  $\tilde{a} = (0.134 - 1.21)10^{-4}A$  is the asymptotic (at large  $E^*$ ) value of the level-density parameter.

As is shown in Refs. 40, 58, and 112, pre-equilibrium emission of particles from the residual nucleus has a strong influence on the fissility of medium nuclei. Such nuclei fission in the first stages of the evaporation cascade, when the compound nucleus still has a high excitation energy. Emission of a pre-equilibrium particle significantly reduces the excitation energy of the compound nucleus and, therefore, reduces the probability of its fissioning. It follows from Fig. 25 that inaccuracies in the description of the thermalization in the residual nucleus can significantly change the fissility of medium and light nuclei. In the region of nuclei with  $A \sim 150-170$ , to compensate the decrease in the fissility it is necessary to take the larger value  $a_f/a = 1.2$ .

However, in the region of nuclei with  $Z^2/A \leq 27$ , the calculated fissilities are lower than the experimental values. The inaccuracies of the model noted above can only increase this discrepancy. The discrepancy can

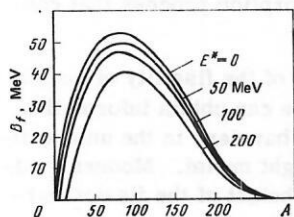


FIG. 27. Variation in the height of the fission barrier of nuclei along the  $\beta$ -stability line in the liquid-drop model with increasing excitation energy of the nuclei.

be attributed to the fact that the parameters of the liquid-drop model are fixed with insufficient reliability. This leads to large values of  $B_f$  on extrapolation to the unknown region of light and medium nuclei. In the model of Refs. 115 and 118, the maximal fission barrier is  $B_f^{\text{max}} \approx 52$  MeV, and in the model of Ref. 119 it is  $B_f^{\text{max}} \approx 56$  MeV (see Fig. 25). To obtain a better description of the experimental fissilities, preference should be given to the modified liquid-drop model of Ref. 120, in which  $B_f^{\text{max}} \approx 43$  MeV.<sup>5)</sup> Such a decrease in the fission barriers leads to an increase in the probability of fission of light and medium nuclei by pions by a factor of about 50 (see Fig. 26).

Another physical effect that could eliminate the discrepancy is the decrease in the fission barrier with increasing excitation energy. Calculations made by the Thomas-Fermi<sup>122</sup> and Hartree-Fock<sup>123</sup> methods predict that "thermal" effects must lead to a lowering of  $B_f$ . This lowering is most appreciable in medium and light nuclei at excitation energies exceeding 50 MeV (Fig. 27). Thermal effects can lead to an increase in the fissility of nuclei with  $Z^2/A \leq 27$  by approximately a factor 10 (see Fig. 26).

Measurement of fission of nuclei by slow  $\pi^-$  mesons makes it possible to verify another prediction of the liquid-drop model—the existence of a critical point  $(Z^2/A)_{\text{cr}}$ , at which the process of fission in light nuclei gives way to a process such as fragmentation. The liquid-drop model of Refs. 115 and 118 determines the position of the critical point at  $(Z^2/A)_{\text{cr}} = 19.8$ , while in the modified liquid-drop model of Ref. 120 it is at  $(Z^2/A)_{\text{cr}} = 32.0$ . Verification of this prediction requires the use of a more reliable experimental method, in which one should measure in coincidence the kinetic energies of the produced fragments.

**Search for Delayed Fission.** The development of theoretical ideas about the structure of the fission barrier has led now to a better understanding of fission.

After capture of a pion, one can have fission of not only highly excited nuclei but also residual nuclei with low excitation energy. The fission of weakly excited nuclei is sensitive to various details of the surface potential energy and, in particular, to the existence of a second minimum in the actinides.<sup>124</sup> The structure of the fission barrier is more clearly manifested in the fission of the neutron-deficient isotopes of the actinides.<sup>125</sup>

The double-humped form of the fission barrier leads to the existence of delayed fission. For example, at Dubna in reactions with heavy ions spontaneously fissioning isomers were discovered<sup>170</sup> and (later) delayed fission was observed.<sup>126</sup> At present, intensive investigations are being made of this phenomenon by means of the various particles  $\gamma$ ,  $n$ ,  $p$ ,  $d$ ,  $\alpha$  and heavy ions. In the study of fission induced by negative muons, delayed

<sup>4)</sup>It is of interest to make observations to observe fragmentation of nuclei by pions<sup>117</sup> in the region of low energies.

<sup>5)</sup>The greatest difficulties in the description of the experimental fissilities of light and medium nuclei are encountered in the so-called droplet model, which estimates the maximal height of the fission barrier at  $B_f^{\text{max}} \approx 80$  MeV (Ref. 121).

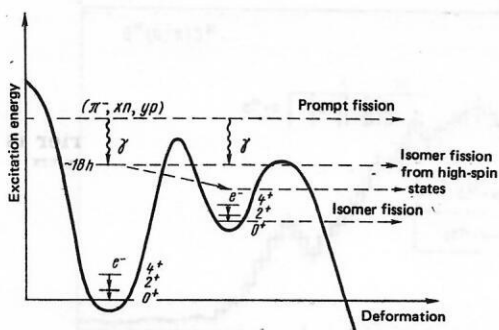


FIG. 28. Fission barrier of nuclei with allowance for shell effects.

fission of the nucleus  $^{238}\text{U}$  has been discovered,<sup>127</sup> this being due to the excitation of the nucleus after capture of a negative muon from an orbit of the  $\mu$ -mesic atom of  $^{237}\text{Np}$ .

The discovery at Dubna of the excitation of high-spin nuclear states<sup>34</sup> as a result of the capture of slow  $\pi^-$  mesons made it possible to begin a search for isomer fission from these high-spin states (Fig. 28).

The search for delayed fission based on the absorption of slow  $\pi^-$  mesons by the  $^{232}\text{Th}$  and  $^{238}\text{U}$  isotopes was made in a wide range of time intervals from tens of nanoseconds to tens of hours.<sup>128</sup> In the time interval from nanoseconds to minutes, the effect was sought by means of a multilayer ionization fission chamber,<sup>129</sup> which makes it possible to make measurements simultaneously with two fissioning substances:  $^{232}\text{Th}$  (0.5 g) and  $^{238}\text{U}$  (0.5 g of natural uranium). Delayed fission in the time interval from minutes to hours was sought by means of Dacron dielectric detectors.

In the nanosecond range, the investigations were made within the pulses of the accelerated particles and the search for the effect was governed by the speed of response of the fission chamber, which is greater than 10 nsec. Figure 29 shows the time distribution of the fissions of the isotope  $^{238}\text{U}$ . One can clearly discern two fission processes: prompt fission at the time of stopping of the  $\pi^-$  meson in the target and delayed fission (the uniformly distributed events to the right of the prompt-fission peak). With allowance for the background, the upper limit for the effect is  $2 \times 10^{-5}$ .

The search for the effect in the millisecond range was made between the pulses of the accelerated particles in the ordinary regime of the accelerator (frequency 166.5

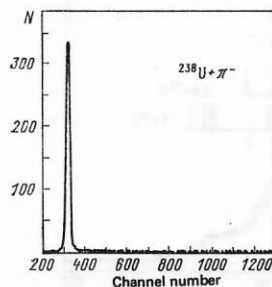


FIG. 29. Time spectrum of fission obtained in coincidence with stoppings of  $\pi^-$  mesons in a target of natural uranium (channel width 0.3 nsec).

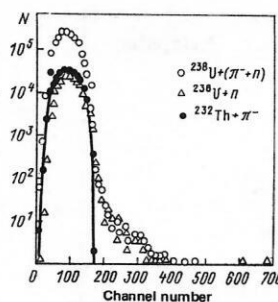


FIG. 30. Time spectrum of fission obtained by irradiation with  $\pi^-$  of a target of natural uranium (channel width 4  $\mu\text{sec}$ ).

Hz). The time selection of the fission events was made by means of a 1024-channel analyzer working in the multiscaler regime (channel width 4  $\mu\text{sec}$ ).

The time distribution of the fission events after summation over ten channels is shown in Fig. 30. It can be seen that besides the prompt fission of  $^{238}\text{U}$  one observes a delayed component with decay time of 150  $\mu\text{sec}$ . In the case of  $^{232}\text{Th}$ , delayed fission was not observed. When allowance is made for the background effects, the upper limit to the delayed-fission effect is  $3.2 \times 10^{-6}$ .

To obtain a more reliable indication of the existence of delayed fission by the reaction products from the absorption of  $\pi^-$  mesons by the  $^{238}\text{U}$  nucleus, more accurate experiments with realization of better background conditions are required. There is no doubt that such investigations are possible in the meson factories.

## 7. SINGLE-NUCLEON AND $\alpha$ -PARTICLE MECHANISMS OF ABSORPTION OF SLOW $\pi^-$ MESONS

*Single-Nucleon Mechanism of Absorption of Slow Pions.* During the last two decades, the question of the single-nucleon mechanism of pion absorption has become the subject of greater interest. One can name at least three reasons for this.

In the first place, single-nucleon absorption of a pion may become a tool to elucidate the part played by the high-momentum component of the nuclear wave function. This reaction can also be used to study single-hole states in residual nuclei.

The particular interest in this reaction is due to the problem of the existence in nuclear matter of a  $\pi$ -meson condensate.<sup>132, 174</sup> Measurements of single-nucleon absorption may be a critical experiment to establish whether a condensate exists in nuclear systems. In the extreme case, one could say more definitely what is the region of existence of nuclei with anomalous density.

Finally, by studying the probability of nonradiative absorption of  $\pi^-$  mesons in nuclei, one can study the problem of whether  $\Delta^{++}$  baryon resonances exist in the ground state of nuclei.

As we have already noted in Sec. 1, in calculations based on two-nucleon absorption of pions it is not possible to describe with sufficient accuracy the high-energy part of the neutron spectrum (see Fig. 2). This fact indicates a possible contribution of the single-nucleon

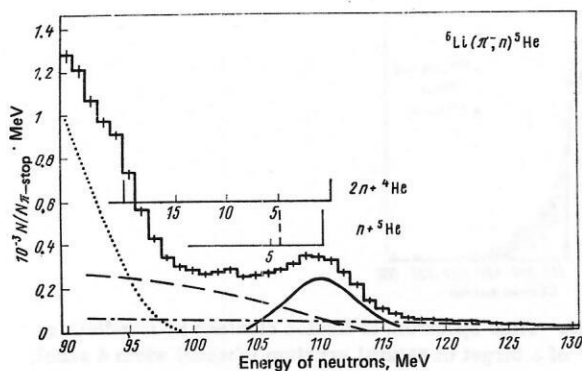


FIG. 31. Spectrum of neutrons obtained after absorption of pions by  ${}^6\text{Li}$  nuclei (histogram). The chain curve is the background from random coincidences; the broken curve is the contribution from the reaction  $(\pi^-, 2n)$  with production of  ${}^4\text{He}$  in the ground state, and the dotted curve is the contribution when  ${}^4\text{He}$  is in the excited state with energy 20 MeV. The peak corresponding to the emission of one nucleon has a Gaussian profile (the continuous curve).<sup>130</sup>

mechanism of pion absorption. In the tail of the high-energy part of the neutron spectrum one can expect the manifestation of structure associated with single-nucleon absorption.

Convincing results on single-nucleon absorption were obtained recently in Ref. 130, in which an investigation was made into the high-energy part of the spectrum of neutrons resulting from absorption of  $\pi^-$  mesons by the nuclei  ${}^6\text{Li}$ ,  ${}^7\text{Li}$ ,  ${}^9\text{Be}$ ,  ${}^{10}\text{Be}$ ,  ${}^{12}\text{C}$ , and  ${}^{14}\text{N}$ . In the case of  ${}^6\text{Li}$ ,  ${}^7\text{Li}$ , and  ${}^{12}\text{C}$ , clear peaks were found in the neutron spectrum in Ref. 130, corresponding to emission of one neutron at the level  $2 \times 10^{-3}$  per one stopped pion (Figs. 31–34).

It follows from Ref. 130 that the measured probability of single-nucleon absorption is  $\sim 10^{-3}$ , and this means that in light nuclei there is no condensate.

The theory developed in Refs. 131 and 132 indicates that the existence of a condensate is most probable in the region of heavy nuclei. The calculations made in Ref. 133 show that in heavy nuclei the presence of a condensate can lead to an increase in the probability of single-nucleon absorption of pions by a factor  $\sim 1000$ .

However, for medium and heavy nuclei, because of the high density of nuclear states in the residual nuclei,

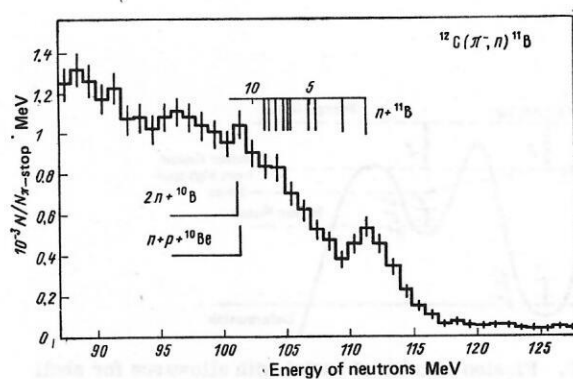


FIG. 33. Spectrum of neutrons obtained in the reaction  ${}^{12}\text{C}(\pi^-, n){}^{11}\text{B}$  (Ref. 130).

it does not appear possible to determine the probability of single-nucleon absorption by measuring the inclusive spectra of the neutrons, as was done in Ref. 130. Already for the nucleus  ${}^{14}\text{N}$  (Fig. 34), the contribution from the excited states of  ${}^{13}\text{C}$  and other reactions ( $2n + {}^{12}\text{C}$ , etc.) prevents separation of the peak corresponding to emission of a single nucleon.

The probability of single-nucleon absorption can be more accurately determined by means of the activation method discussed in the previous sections.

In Ref. 134, a search was made for a high-spin hafnium isomer  ${}^{180\text{m}}\text{Hf}$ . One of the important assumptions made in Ref. 134 is that single-nucleon capture occurs, like two-nucleon capture, in the surface layer of the nucleus. In contrast, the phenomenon of pion condensation has a volume nature.<sup>132, 133</sup> Nevertheless, the calculations of Ref. 133 show that the probability of single-nucleon absorption is sensitive to the existence of a pion condensate in heavy nuclei. In Fig. 35, which is taken from Ref. 133, we have plotted the probability of nucleon emission as a function of the condensate radius in the case of absorption of a  $\pi^-$  meson from the  $4f$  level in lead. If it is assumed that the region of existence of the condensate extends to the nuclear-matter density  $0.7\rho_0$  ( $\rho_0$  being the density of nucleons at the center of the nucleus), the presence of the condensate will increase the probability of single-nucleon emission by a factor of approximately 100.

Thus, it is to be expected that when slow pions are captured high-spin isomers are produced with high

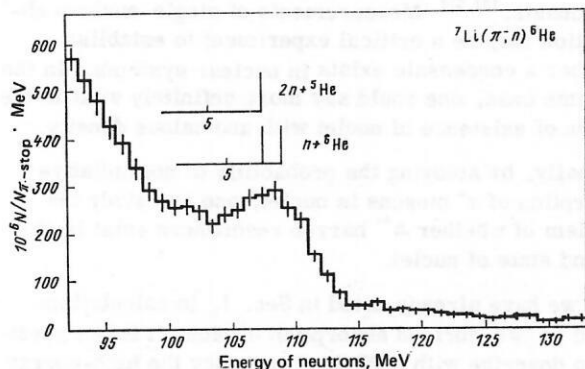


FIG. 32. Spectrum of neutrons obtained after absorption of pions by  ${}^7\text{Li}$  nuclei.<sup>130</sup>

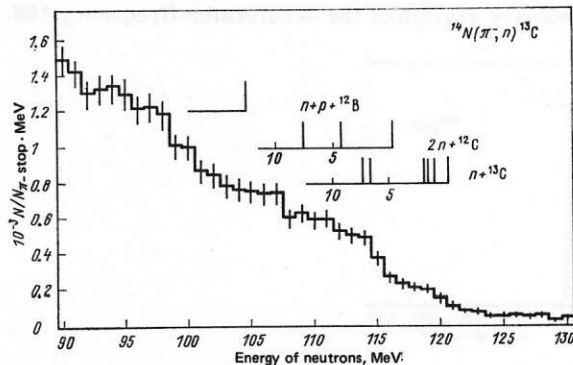


FIG. 34. Spectrum of neutrons obtained in the reaction  ${}^{14}\text{N}(\pi^-, n){}^{13}\text{C}$  (Ref. 130).



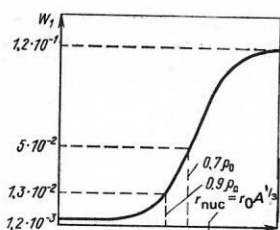


FIG. 35. Dependence of the probability of emission of one nucleon as a result of absorption of slow pions from the 4f level for  $^{207}\text{Pb}$  on the radius of the condensate.

probability through the emission from the nucleus of one fast nucleon. In particular, among the products of the  $^{181}\text{Ta}(\pi^-, n)$  reaction there must be formed  $^{180\text{m}}\text{Hf}(I^\pi = 8^-)$ . The choice of a high-spin isomer as final product is also made in order to reduce the contribution from radiative capture of the pion with subsequent emission of one neutron, since for the radiative capture  $\pi^- + p \rightarrow \gamma + n$  the  $\gamma$  ray with energy of about 100–120 MeV cannot lead to an angular momentum of the residual nucleus  $M = E_\gamma r_{\text{nuc}}/c$  greater than  $8\hbar$  ( $r_{\text{nuc}}$  is the radius of the nucleus). The spin of the initial nucleus  $^{181}\text{Ta}$  is  $7/2$ , and the orbital angular momentum of the pion is  $3\hbar$ , and therefore the total angular momentum of the  $\gamma$  ray, the initial nucleus, the pion, and the slow neutron is inadequate for population of the high-spin state of  $^{180\text{m}}\text{Hf}$  with  $I^\pi = 8^-$ .

In Fig. 36, we show part of the  $\gamma$ -ray spectrum of the hafnium isotopes produced by the capture of pions by the nucleus  $^{181}\text{Ta}$ . The decay scheme of  $^{180\text{m}}\text{Hf}$  has been well studied, and if this isomer state were populated in the reaction  $^{181}\text{Ta}(\pi^-, n)$ , one could note in the  $\gamma$ -ray spectrum the strongest and cleanest  $\gamma$ -ray lines at 443.2 keV (84%) and 500.7 keV (13%) from the decay of this isomer (in Fig. 36, they are indicated by the arrows).

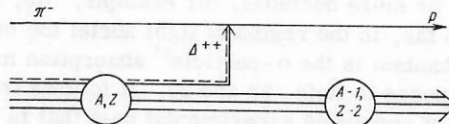
The low probability ( $\sim 10^{-5}$ ) of population of the high-spin  $^{180\text{m}}\text{Hf}$  isomer in the reaction  $^{181}\text{Ta}(\pi^-, n)$  speaks for a dominant role of the two-nucleon absorption mechanism. In addition, if there is indeed a unique connection between the single-nucleon pion absorption mechanism and a condensate of the nucleus, the obtained result indicates that in heavy nuclei a condensate is also not

realized.

Thus, the process of single-nucleon pion absorption in the form of the reaction  $\pi^- + p \rightarrow n$  is strongly suppressed compared with the two-nucleon pion absorption.

We consider one further interesting possibility leading to single-nucleon emission; this is related to the idea that there exist virtual excited nucleons in the ground state of a nucleus. In Ref. 135, to explain the discrepancy between the experimental and theoretical values of the interaction cross sections of protons scattered forward by deuterons, it was suggested that there could be virtual excited nucleons (isobars) in the ground state of nuclei. In Ref. 136, in which an investigation was made into the scattering of 15-GeV pions by deuterons, observation of events in a bubble chamber that indicate the existence of a  $\Delta^{++}$  component in the deuteron is reported. According to the estimates made in Ref. 136, the probability of such virtual  $\Delta^{++}$  components in the deuteron is  $\sim 0.7\%$ . Subsequently, Refs. 137–140 were devoted to the investigation of this question.

In principle, the existence in nuclei of the  $\Delta^{++}$  isobar can be manifested in the  $(\pi^-, p)$  reaction in accordance with the diagram



There is only one experimental study known<sup>137</sup> in which the probability of the reaction  $^{12}\text{C}(\pi^-, p)^{11}\text{Be}$  was determined by means of the activation method. The obtained probability  $W_1 = (4.5 \pm 0.8) \times 10^{-4}$  is evidently overestimated because of the accompanying reaction  $^{13}\text{C}(n, 2p)^{11}\text{Be}$ .

In Ref. 139, a study is made of the probability of single-proton emission in the reaction  $(\pi^-, p)$  on a single-isotope  $^{133}\text{Cs}$  target (Fig. 37). The probability of the reaction  $^{133}\text{Cs}(\pi^-, p)^{132}\text{I}$  is deduced from the yield of  $\gamma$  rays of the  $^{132}\text{I}$  isotopes. The probability obtained for this reaction is  $W_1 = (5.0 \pm 0.5) \times 10^{-4}$ . The background from the reaction  $^{133}\text{Cs}(n, 2p)^{132}\text{I}$  was checked specially (Fig. 38). In the background spectrum,  $\gamma$  rays from  $^{132}\text{I}$  were not found.

Additional experiments to investigate the probability of single-proton emission were made using a single-

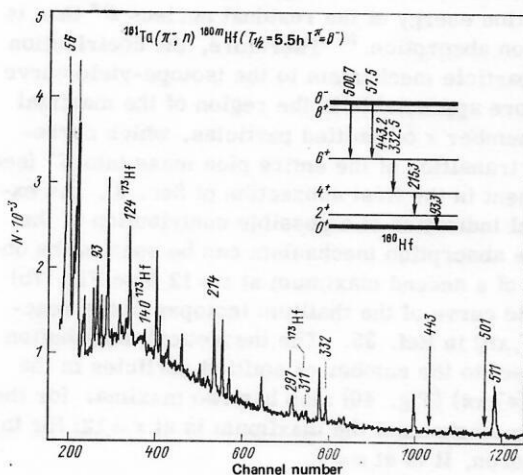


FIG. 36. Part of the  $\gamma$ -ray spectrum of the hafnium isotopes produced after absorption of pions in a tantalum target.

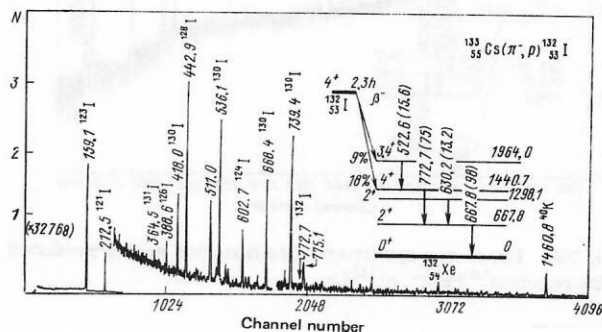


FIG. 37. The  $\gamma$ -ray spectrum of iodine isotopes produced after absorption of pions in a  $^{133}\text{Cs}$  target.

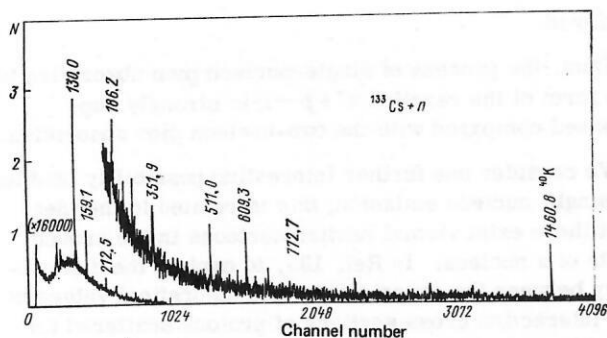


FIG. 38. The  $\gamma$ -ray spectrum of radioactive nuclei produced by irradiation with neutrons of a cesium target.

isotope  $^{141}\text{Pr}$  target (Fig. 39). The probability of the reaction  $^{141}\text{Pr}(\pi^-, p)^{140}\text{La}$  is  $3 \times 10^{-4}$ .

In the future, it is planned to make an experimental investigation realizing better background conditions with a view to measuring the cross-section ratio  $\sigma(\pi^-, p)/\sigma(\pi^-, n)$ , which according to the estimates of Refs. 133 and 142 is approximately 1/20.

**The  $\alpha$ -Particle Mechanism of  $\pi^-$  Absorption.** In principle, mesons can be absorbed by not only two but also three, four, or more nucleons, for example,  $^3\text{He}$ ,  $^4\text{He}$ ,  $^4\text{Li}$ , etc. So far, in the region of light nuclei the most studied mechanism is the  $\alpha$ -particle<sup>6)</sup> absorption mechanism proposed in Refs. 28 and 29. It follows from the analysis of numerous experimental data that in light nuclei the probability of such absorption is  $\sim 20$ – $30\%$ , while that of two-nucleon absorption is  $70$ – $80\%$ .<sup>4</sup> In the region of medium and heavy nuclei, the part played by the  $\alpha$ -particle mechanism has not yet been studied, although here too it may be asserted that the two-nucleon mechanism is predominant.

At present, we know of only one paper<sup>40</sup> in which an estimate has been made of the contribution of the  $\alpha$ -particle mechanism of pion absorption by complex nuclei. In the case of the absorption of a pion by a free  $\alpha$  particle, three reaction channels are possible; these have the following relative probabilities  $W$ :

$$\pi^- + {}^4\text{He} \rightarrow t + n, \quad W_2 = (19 \pm 1)\% \text{ (Refs. 171 and 172),} \quad (16a)$$

$$\pi^- + {}^4\text{He} \rightarrow d + 2n, \quad W_3 = (58 \pm 7)\% \text{ (Ref. 173),} \quad (16b)$$

$$\pi^- + {}^4\text{He} \rightarrow p + 3n, \quad W_4 = (26 \pm 6)\% \text{ (Ref. 173).} \quad (16c)$$

One cannot directly use these probabilities to calculate  $\alpha$ -particle absorption in nuclear matter, if for no other reason than that when a pion is absorbed by the  $^4\text{He}$  nucleus in vacuum the two-nucleon mechanism must make a contribution. On the basis of these considerations, to determine the maximal effect in Ref. 40 it was assumed as a simplification that after the absorption there is realized only channel (16c) with four particles in the final state. In the sense of the kinematics, the reaction (16c) is an extreme reaction relative to the reaction (4), since in it, after the absorption, the pion mass is transformed into the kinetic energy of four, and not two nucleons.

The nucleons produced in the reaction (16c) will have lower energies than in the reaction (4), and will be absorbed with greater probability by the target nucleus. As a result, this channel of  $\alpha$ -particle absorption is more effective in transforming the pion mass  $m_\pi$  into the excitation energy of the residual nucleus  $E^*$  than is two-nucleon absorption.<sup>40</sup> Therefore, the contribution of the  $\alpha$ -particle mechanism to the isotope-yield curve will be more appreciable in the region of the maximal possible number  $x$  of emitted particles, which corresponds to transition of the entire pion mass into  $E^*$  (see our comment in the first subsection of Sec. 3). An experimental indication of a possible contribution of the  $\alpha$ -particle absorption mechanism can be seen in the observation of a second maximum at  $x=12$  (see Fig. 7b) in the yield curve of the thallium isotopes in the reaction  $\text{Pb}(\pi^-, xn)$  in Ref. 35. The theoretical distribution with respect to the number of emitted particles in the reaction  $(\pi^-, xn)$  (Fig. 40) also has two maxima: for the  $\alpha$ -particle mechanism the maximum is at  $x=12$ ; for the quasideuteron, it is at  $x=7$ .

To determine the part played by the  $\alpha$ -particle absorption mechanism, it is important to make a more

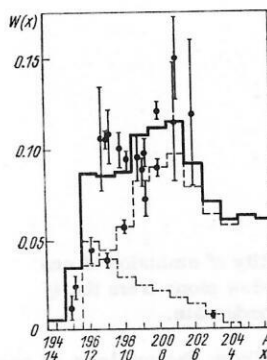


FIG. 40. Distribution with respect to the multiplicity of the emitted neutrons in the reaction  $^{208}\text{Pb}(\pi^-, xn)^{108-x}\text{Tl}$ . The black circles are from the experiment of Ref. 35; the broken line is a calculation in accordance with the two-nucleon absorption mechanism<sup>40</sup>; the chain curve is a calculation in accordance with the  $\alpha$ -particle absorption mechanism; the solid line is the calculation under the assumption that in 25% of the cases the pion is absorbed by an  $\alpha$  cluster and in 75% of the cases by a pair of nucleons.

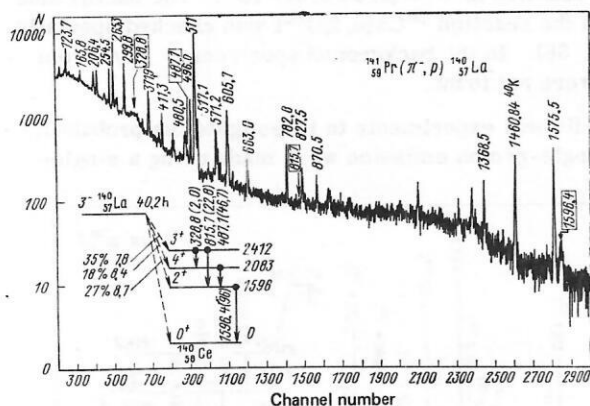


FIG. 39. The  $\gamma$ -ray spectrum of radioactive nuclei produced in the reaction  $^{141}\text{Pr}(\pi^-, p)^{140}\text{La}$ .

<sup>6)</sup>In what follows, for brevity, we shall use the expression " $\alpha$ -particle" instead of the words "four independent nucleons."

detailed investigation of the isotope yields when there is a large number of emitted neutrons for heavy nuclei with  $A \approx 200$ . These investigations are fairly complicated, since such isotopes are characterized by low yields and short lifetimes.

Another source of information about the  $\alpha$ -particle absorption mechanism is the spectra of complex charged particles ( $d, t$ ), to which the channels (16a) and (16b) can contribute (see the second subsection of Sec. 2). It would therefore be desirable to generalize the simplified treatment of  $\alpha$ -particle absorption in Ref. 40 by including in the model the channels with two and three particles in the final state. This would make possible a more detailed analysis of the latest experimental data<sup>64,66</sup> on the yield of complex charged particles.

As is shown by the calculations of Refs. 40 and 58, the excitation of high-spin states must also be observed in the  $\alpha$ -particle mechanism. Of particular interest is the channel (16a) with two particles in the final state. In this case, the triton energy in the center-of-mass system will be  $E_t \approx 35$  MeV and the neutron energy  $E_n \approx 105$  MeV. Therefore, a neutron of such high energy will be emitted from the surface layer of the nucleus and the absorption in the nucleus of the comparatively slow triton must be accompanied by approximately 1.25 times larger values of the angular momenta of the residual nuclei than in the case of quasideuteron absorption. In this case, there is formed a residual nucleus with excitation energy  $E^* \approx 30$  MeV, and therefore the dependence of the mean angular momentum on the number of emitted particles will have a maximum, not at  $x = 7$  as in the case of the quasideuteron mechanism, but at  $x \approx 4$ .

Thus, already the example of  $\alpha$ -particle absorption shows that the determination of the parts played by the different many-nucleon absorption mechanisms is a complicated problem, and its solution requires not only new and complicated experiments but also a significant improvement in the existing theoretical models.

## 8. ABSORPTION OF SLOW $\pi^-$ MESONS IN CHEMICAL COMPOUNDS AND MECHANICAL MIXTURES OF ELEMENTS

Hitherto, we have considered the final stage in the process of formation of the  $\pi$ -mesic atom, i.e., how the captured  $\pi^-$  meson is absorbed by the atomic nucleus—by one nucleon, a pair of nucleons, or a many-nucleon association. However, it is of no less interest to study the initial stage in the formation of the  $\pi$ -mesic atom, which begins with the process of deceleration of the mesons in the matter. That the probability of production of mesic atoms may depend on the type of matter in which the mesons are stopped was first pointed out by Fermi and Teller.<sup>141</sup> They predicted that the probability of meson capture by individual elements of a chemical compound would be proportional to the charge  $Z$  of the nucleus and the concentration of the atoms. This is known as the  $Z$  law.

Such investigations into the structure of chemical compounds by means of  $\mu$  mesons, which has received

the name of mesochemistry, are carried out intensively in all laboratories of the world. In this section, we wish to consider a new method in mesochemistry for determining the relative probability of production of  $\pi$ -mesic atoms in chemical compounds by means of the induced radioactivity of the residual nucleus. This method is based in the first place on the fact that pions, in contrast to muons, have equal probabilities of atomic and nuclear capture. In addition, after activation of the chemical compound by the  $\pi^-$  mesons, the products of the reaction on one nucleus are readily distinguished from the products of the reaction on the other nucleus if these two nuclei of the compound differ in  $Z$  by at least a few units. The yield of the reaction products is determined from the strongest  $\gamma$ -ray lines of the produced residual nucleus by means of the activation method described in Sec. 3. A final advantage of the method is that it is much easier to investigate high-energy nuclear  $\gamma$  transitions (for which a high resolution is not required and the intensity can be more readily determined) than medium-energy x-ray transitions, as was attempted earlier.

Before we turn to the direct experimental investigations using this method, let us consider the situation with regard to the  $Z$  law. The  $Z$  law has frequently been verified experimentally for a number of chemical compounds.<sup>142-148</sup> The results of all these experiments show that a simple  $Z$  dependence valid for all compounds does not exist.<sup>3,149</sup>

For example, let us consider the experiments in which the probability of atomic capture of negative muons in binary compounds and oxides were determined<sup>150,151</sup> on the basis of the intensity of the muonic x-ray radiation of the  $K$  series from one of the elements in the pure state and from the same element in a compound. It was shown that the ratio of the probabilities of atomic capture in compounds of metals with halogens and in alloys of metals can be described by the linear dependence  $0.66Z_1/Z_2$ , while the probability of atomic capture of muons in oxides varies periodically with increasing  $Z$ . The features of  $\mu$ -atomic phenomena in chemical compounds were investigated in Refs. 152-156.

Chemical effects in pionic atoms were studied in Refs. 157-161.

In Ref. 162, there is proposed a dependence that differs from the one given above for the probability of atomic capture of mesons on the atomic number; according to this, the ratio of the probabilities for capture by atoms  $Z_1$  and  $Z_2$  is

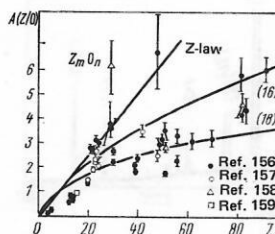


FIG. 41. Relative probabilities of atomic capture of mesons in oxides.<sup>164</sup>



$$A(Z_1/Z_2) = Z_1^{1/3} \ln(0.57Z_1)/Z_2^{1/3} \ln(0.57Z_2). \quad (16)$$

It is shown in Refs. 163 and 164 that the ratio of the probabilities of pion capture by  $Z$  atoms and hydrogen atoms is

$$A(Z/H) = (7.1 \pm 0.4)(Z^{1/3} - 1), \quad (17)$$

and in the general case for binary systems

$$A(Z_1/Z_2) = (Z_1^{1/3} - 1)/(Z_2^{1/3} - 1). \quad (18)$$

The available experimental data on the atomic capture of  $\mu^-$  and  $\pi^-$  mesons are analyzed in Ref. 164. The value of  $\chi^2$  is used as a criterion of the agreement between experiment and the considered dependences (Fig. 41). It is asserted that both the  $Z^{1/3}$  dependences [(16) and (18)] give a significantly better description of the results of the experiments than the  $Z$  law. However, it should be noted that the majority of the experimental data were obtained for compounds containing hydrogen, and the data on the relative probability of production of pionic atoms in chemical compounds of heavier elements are very sparse. In addition, because of the strong pion-nucleus interaction, which influences the pionic x-ray radiation of the lowest transitions, it was not possible to measure transitions between low-lying states of the pionic atom. Only the relative intensities of the x rays emitted when a pion makes a transition between high-lying levels were investigated in Refs. 155 and 156.

The study of the extensive class of compounds containing hydrogen is undoubtedly important, but from the point of view of elucidating the general picture of pionic chemistry it is necessary to extend the number of investigated compounds and increase the accuracy of the experimental data.

In Ref. 165, iodides of alkali metals were investigated by the activation method. In the investigated compounds, LiI, NaI, KI, RbI, and CsI, the ionic bonds are almost identical, which makes it possible to follow the

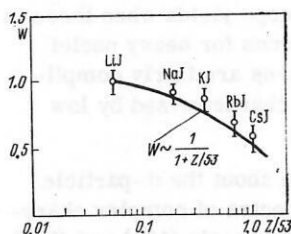


FIG. 43. Relative probability of atomic capture of pions in iodides of alkali metals. The solid curve is the prediction of the  $Z$  law, and the open circles are the data of Ref. 165.

influence of only the charge of the nucleus on the probability of production of a mesic atom.

If the conditions of irradiation and measurement are identical, one can investigate the influence of atoms of the alkali metals on the yield of Sb isotopes when  $\pi^-$  mesons are absorbed by the iodine nucleus.

The relative probability of nuclear absorption of negative pions in these chemical compounds can be determined from the yield of the high-spin isomer  $^{116m}\text{Sb}$  ( $T = 8^-, T_{1/2} = 60$  min), which is formed in the reaction  $^{127}\text{I}(\pi^-, 1p, 10n)^{116m}\text{Sb}$ . In Fig. 42, we show sections of the  $\gamma$ -ray spectrum of the antimony and lead isotopes produced by the absorption of pions in LiI, NaI, KI, and CsI targets.

The results of the experiment showed that for this type of compounds the Fermi-Teller  $Z$  law is satisfied; according to it, the probability of production of a mesic atom in the chemical compounds is proportional to the charge of the nucleus. This can be clearly seen in Fig. 43, in which we have plotted the probability of production of mesic atoms in the chemical compounds LiI, NaI, KI, RbI, and CsI.

Usually, to study the influence of the chemical bond on the probability of atomic capture of mesons one compares the probability of production of mesic atoms in chemical compounds of the elements and corresponding mechanical mixtures.

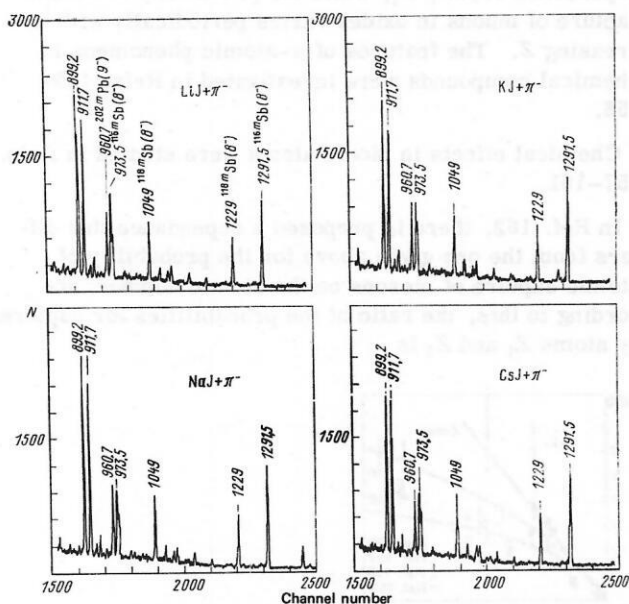


FIG. 42. Sections of the  $\gamma$ -ray spectra of antimony and lead isotopes produced after absorption of  $\pi^-$  mesons in LiI, NaI, KI, and CsI targets.

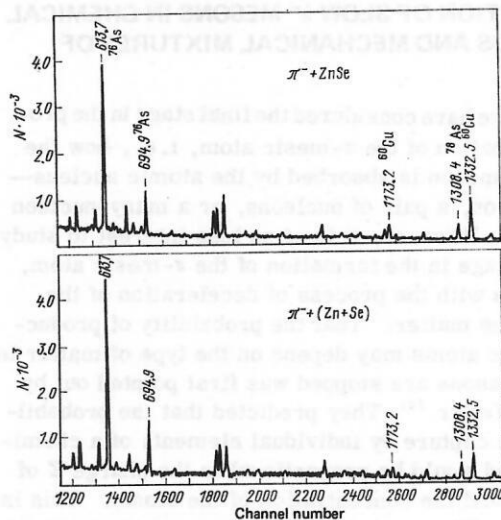


FIG. 44. Sections of the  $\gamma$ -ray spectra of Cu and As isotopes produced after absorption of pions in the chemical compound ZnSe and the mechanical mixture Zn + Se of the elements.

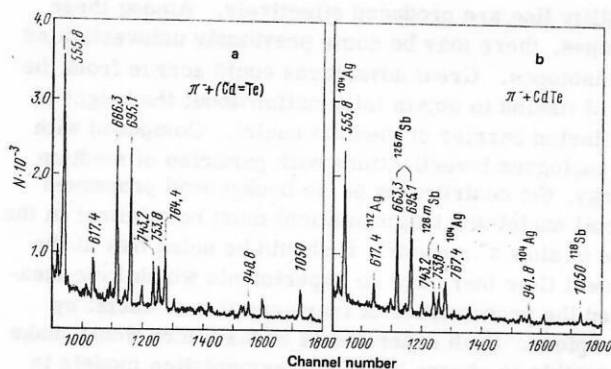


FIG. 45. Sections of the  $\gamma$ -ray spectra of Ag and Sb isotopes produced after absorption of pions in the chemical compound CdTe and the mechanical mixture Cd + Te of the elements.

In pionic atoms of mesochemical compounds, a number of anomalous mesochemical effects have been found. For example, in Ref. 158, in an investigation into the intensity of x-ray emission of pionic atoms in chemical compounds, it was noted that the ratio of the intensities of  $4f-3d$  transitions in Zn and Se is 5.6 times greater for the chemical compound ZnSe than for the mechanical mixture of the same elements. At the same time, the intensity ratios of the  $5g-4f$  transitions in Cd and Te are the same in the chemical compound CdTe and in the mechanical mixture Cd + Te. The reason for such a strong anomalous effect in ZnSe was not explained. First, this effect may be due to the influence of the chemical bond on the probability of production of the mesic atom; second, it may be due to the influence of the chemical bond on the structure of the mesic x-ray series; finally, it may be due to the grain size of the powders in the mechanical mixtures of the elements. Recent calculations made in Ref. 166 show that the grain sizes in mixtures of elements may have a significant influence on the relative probability of formation of mesic atoms.

By means of the same activation method based on measurement of the induced radioactivity of the residual nuclei resulting from the absorption of negative pions, an investigation was made in Refs. 167 and 168 of the chemical compounds ZnSe and CdTe and the corresponding mechanical mixtures. The grain size of the Cd and Te powders in the mechanical mixture of elements Cd + Te was the same and equal to  $10 \mu\text{m}$ , while the grain size of the Se powder in the combination Zn + Se varied from 10 to  $1000 \mu\text{m}$ , the grain size of the

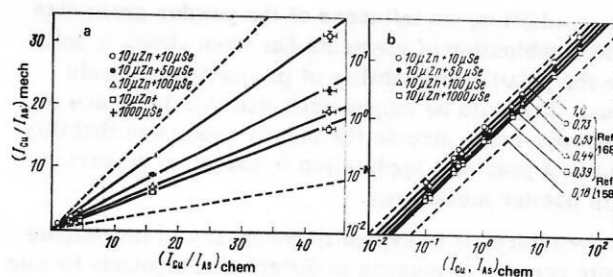


FIG. 47. Ratios of the  $\gamma$ -ray intensities of the Cu and As isotopes produced after absorption of pions in the chemical compound ZnSe (along the abscissa) and in the mixture Zn + Se of the elements (along the ordinate) (a); the same dependence in logarithmic scale (b).

Zn powder being constant and equal to  $10 \mu\text{m}$ .

Under identical conditions of irradiation and measurement of these samples in a  $\pi^-$  beam, the yields of the radioactive isotopes of Ag, Sb, Cu, and As produced by the absorption of pions by the nuclei Cd, Te, Cu, and Se were investigated. In Figs. 44 and 45, we give sections of the  $\gamma$ -ray spectra containing the strongest  $\gamma$  lines of the Ag, Sb, Cu, and Se isotopes.

The ratios of the  $\gamma$  intensities of these isotopes produced in the chemical compounds and in the corresponding mixtures are shown in Figs. 46 and 47a and 47b. It can be seen (see Fig. 46) that the ratio of the probability of formation of mesic atoms in Cd and Te does not depend on the combination (CdTe or Cd + Te). Recall that the grain size of the Cd and Te powders in the mechanical mixture Cd + Te was the same (at  $10 \mu\text{m}$ ). With increasing grain size of one of the powders of the mixture (in the given case, Se; see Figs. 47a and 47b) the probability of pion stoppings in the grains increases. With decreasing size of the powder grains of both elements, the ratio of the probabilities of absorption of pions in the mechanical mixture approaches the probability ratio in the chemical compound. (This can be clearly seen in Fig. 47b on the basis of the slope of the dependence of the  $\gamma$ -intensity ratio of the isotopes of Cu and As.)

Thus, the anomalous effect observed in Ref. 158 is evidently due to the influence of the grain size of the powders on the relative probability of pion absorption in the mechanical mixture of the elements Zn and Se.

It is known that the search for an adequate law of atomic capture of mesons involves many difficulties associated with the influence on the probability of atomic capture of various effects, so that in an investigation of the probability of meson capture by heterogeneous mixtures of elements especial care must be taken.

We note finally that the new method in mesochemistry considered in the present section, in which meson capture is identified by the induced radioactivity of the residual nucleus, has proved to be very promising. Already the first experiments (Refs. 165, 167, and 168) using this method have given good results. It has been shown that the probability of production for the investigated chemical compounds is proportional to the charge of the nucleus, i. e., the Fermi-Teller  $Z$  law is satis-

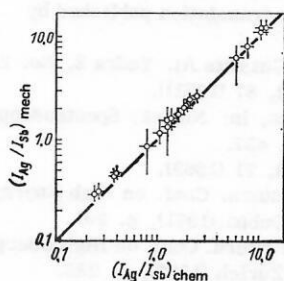


FIG. 46. Ratios of the  $\gamma$ -ray intensities of the Ag and Sb isotopes produced after absorption of pions in the chemical compound CdTe (along the abscissa) and in the mechanical mixture Cd + Te of the elements (along the ordinate).

fied; in addition, an influence of the powder grain size in the combination of elements has been shown to influence the relative probability of production of mesic atoms. It should be emphasized that this influence of the powder grain size on the meson capture probability could find practical application in industry, in particular in powder metallurgy.

In the future, it is evidently necessary to investigate atomic capture of mesons in different compounds by one and the same method, for example, the activation method. It is to be expected that such investigations will remove the contradictions and that the method indicated above for determining the relative probability of nuclear absorption of pions in chemical compounds on the basis of the induced radioactivity of the residual nucleus will take its due place among the other methods of studying the structure of matter.

## CONCLUSIONS

The experiments on the absorption of slow  $\pi^-$  mesons by complex nuclei considered in this review not only augment the analogous investigations made with light nuclei but also make it possible to obtain new and unique information about this process. As an example, we may mention the experiments on the new phenomenon of excitation of high-spin states produced by nuclear capture of pions. At the present time, there is a comparatively small number of established facts indicating two-nucleon absorption of negative pions, and the excitation of high-spin states can be regarded as a further proof. In addition, these experiments have shown that the pion is absorbed in the surface layer of a complex nucleus. The main proof of this can be seen in the established dependence of the probability of excitation of isomers on the number of neutrons emitted after absorption of the pion.

It follows from the analysis of the complete set of experimental data that the two-nucleon mechanism of pion absorption is predominant. The probability of the single-nucleon absorption mechanism in both light and heavy nuclei does not exceed  $10^{-3}$ – $10^{-4}$ . This indicates that in real nuclei a pion condensate does not exist. Later, it would be desirable to make experimental investigations with a view to studying whether excited nucleons ( $\Delta^{++}$  isobars) exist in nuclei.

At present, the question of the contribution of more complicated absorption mechanisms, for example, the  $\alpha$ -particle mechanism, remains open. An indication that such a mechanism does operate in the region of medium and heavy nuclei could be the observation of structure in the isotope-yield curve or the excitation of a high spin of a residual nucleus when only a few (3–5) particles are emitted. The detection of enhancement of the  $\alpha$ -particle mechanism in the region of heavy nuclei would indicate  $\alpha$  clustering in the surface layer of such nuclei.

Reactions in which slow pions are absorbed can be successfully used to investigate the properties of nuclei. In these reactions, because of the strong disintegration of the target nucleus, isotopes far from the  $\beta$ -

stability line are produced effectively. Among these isotopes, there may be some previously uninvestigated new isotopes. Great advantages could accrue from the use of fission to obtain information about the height of the fission barrier of medium nuclei. Compared with the analogous investigations with particles of medium energy, the contribution of the background processes (recoil nuclei and fragmentation) must be minimal in the case of slow  $\pi^-$  mesons. It should be noted that at the present time there are no experiments which have measured the probabilities of fragmentation of nuclei by slow pions. Such experiments in the future would make it possible to choose between fragmentation models in which the large momentum introduced by the incident particle is the determining factor and the models in which the high excitation energy of the residual nuclei is the dominant factor.

The discovery of excitation of high-spin isomer states after capture of slow  $\pi^-$  mesons means that one can also start to look for fission of heavy isotopes in these isomer states. There is no doubt that such experiments could yield valuable information about both the height of the fission barrier and the structure of the high-spin states.

The method of studying the mechanism of pion absorption by nuclei through investigating the effect of the rotational motion of the residual nuclei can also be extended to other nuclear reactions. Since large values of the angular momenta of the residual nuclei are associated with the emission of fast particles from the surface layer of the nucleus, one can expect the excitation of high-spin states as a result of the absorption of  $K^-$  mesons and antiprotons by complex nuclei. It may be hoped that such experiments will become possible in the near future and that they will give valuable information about the mechanism of nuclear absorption of these particles.

We should like to thank Professors V. M. Lobashev and M. G. Meshcheryakov for constant interest in the work, I. S. Batkin, R. Ya. Zul'karneev, and G. G. Bunatyan for helpful discussions and valuable comments, and also B. Kornitskaya for assistance in writing the review.

<sup>1</sup>G. Backenstoss, *Ann. Rev. Nucl. Sci.* **20**, 467 (1970); *Usp. Fiz. Nauk* **107**, 405 (1975).

<sup>2</sup>J. Hüfner, *Phys. Rep.* **C21**, 1 (1975).

<sup>3</sup>Y. N. Kim, *Mesic Atoms and Nuclear Structure*, North-Holland, Amsterdam (1971) [Russian translation published by Mir (1975)].

<sup>4</sup>T. I. Kopaleishvili, *Fiz. Elem. Chastits At. Yadra* **2**, No. 2, 439 (1971) [*Sov. J. Part. Nucl.* **2**, 87 (1971)].

<sup>5</sup>D. K. Anderson and D. A. Jenkins, in: *Nuclear Spectroscopy and Reactions*, London (1974), p. 457.

<sup>6</sup>D. S. Koltun, *Adv. Nucl. Phys.* **3**, 71 (1969).

<sup>7</sup>D. S. Koltun, in: *Proc. Fourth Intern. Conf. on High Energy Physics and Nuclear Structure*, Dubna (1971), p. 201.

<sup>8</sup>H. K. Walter, in: *Proc. Seventh Intern. Conf. on High Energy Physics and Nuclear Structure*, Zurich (1977), p. 285.

<sup>9</sup>I. Becker and Yu. A. Batusov, *Riv. Nuovo Cimento* **1**, 309 (1971).

<sup>10</sup>V. V. Balashov, G. Ya. Korenman, and R. A. Éramzhyan, *Pogloshchenie mezonov atomnymi yadrami* (Absorption of



- Mesons by Nuclei), Moscow (1978).
- <sup>11</sup>D. Perkins, Phys. Mag. 40, 601 (1969).
  - <sup>12</sup>V. De Sabbata, E. Manaresi, and G. Puppi, Nuovo Cimento 9, 726 (1952); 10, 1704 (1953).
  - <sup>13</sup>M. Demeur, A. Huleus, and G. Vanderhaeghe, Nuovo Cimento 4, 509 (1956).
  - <sup>14</sup>G. A. Azimov *et al.*, Sov. Phys. 4, 632 (1957).
  - <sup>15</sup>G. Brown and I. S. Hughes, Phys. Mag. 2, 777 (1957).
  - <sup>16</sup>A. O. Vaisenberg, E. D. Kolganova, and N. V. Rabin, Zh. Eksp. Teor. Fiz. 47, 1262 (1964) [Sov. Phys. JETP 20, 854 (1964)].
  - <sup>17</sup>A. Alumkal *et al.*, Nuovo Cimento 17, 316 (1964).
  - <sup>18</sup>H. L. Anderson *et al.*, Phys. Rev. B 133, 392 (1964).
  - <sup>19</sup>G. Venuti Campos, G. Frenterotta, and G. Matthiae, Phys. Lett. 9, 45 (1964); Nuovo Cimento 34, 1446 (1964).
  - <sup>20</sup>P. M. Hattersley, H. Muirhead, and J. N. Wouds, Nucl. Phys. 67, 309 (1965).
  - <sup>21</sup>V. Tongiorgi Cocconi and D. A. Edwards, Phys. Rev. 88, 145 (1952).
  - <sup>22</sup>L. Winnsberg, Phys. Rev. 95, 198 (1954).
  - <sup>23</sup>A. Turkevich and S. Fung, Phys. Rev. 92, 521 (1953).
  - <sup>24</sup>T. T. Sugichara and W. P. Libby, Phys. Rev. 88, 145 (1952).
  - <sup>25</sup>R. H. Fowler and V. M. Mayes, Proc. Phys. Soc., London, Sect. A 92, 377 (1967).
  - <sup>26</sup>K. H. Bruechner, R. Serber, and K. H. Watson, Phys. Rev. 84, 258 (1951).
  - <sup>27</sup>J. S. Levinger, Phys. Rev. 84, 43 (1951).
  - <sup>28</sup>I. S. Shapiro and V. M. Kolybasov, Zh. Eksp. Teor. Fiz. 44, 270 (1963) [Sov. Phys. JETP 17, 185 (1963)].
  - <sup>29</sup>V. M. Kolybasov, Yad. Fiz. 3, 729, 964 (1966) [Sov. J. Nucl. Phys. 3, 535, 698 (1966)]; V. M. Kolybasov and V. A. Tsepov, Preprint No. 852, ITEP, Moscow (1971).
  - <sup>30</sup>W. Elsaesser and J. M. Eisenberg, Nucl. Phys. A144, 441 (1970).
  - <sup>31</sup>R. S. Kaushal and Y. R. Waghmare, Nucl. Phys. A144, 449 (1970).
  - <sup>32</sup>L. S. Azhgirey *et al.*, Zh. Eksp. Teor. Fiz. 33, 1185 (1957) [Sov. Phys. JETP 6, 911 (1958)].
  - <sup>33</sup>D. H. Wilkinson, in: Proc. Rutherford Jubilee Intern. Conf., Manchester (1961), p. 339.
  - <sup>34</sup>V. S. Butsev *et al.*, in: Tezisy XXV soveshchaniya po yadernoi spektroskopii i strukture atomnogo yadra (Proc. 25th Symposium on Nuclear Spectroscopy and Nuclear Structure), Leningrad (1975), p. 150.
  - <sup>35</sup>V. S. Butsev *et al.*, Preprint R6-8541 [in Russian], JINR, Dubna (1975); Yad. Fiz. 23, 17 (1976) [Sov. J. Nucl. Phys. 23, 8 (1976)].
  - <sup>36</sup>P. Ebersold *et al.*, Phys. Lett. B58, 428 (1975).
  - <sup>37</sup>H. S. Pruijs *et al.*, Helv. Phys. Acta 50, 199 (1977).
  - <sup>38</sup>H. D. Engelhardt, C. W. Lewis, and H. Uelrich, Nucl. Phys. A258, 480 (1976).
  - <sup>39</sup>H. W. Bertini, Phys. Rev. C 1, 423 (1970).
  - <sup>40</sup>A. S. Iljinov, V. I. Nazaruk, and S. E. Chigrinov, Nucl. Phys. A268, 513 (1976).
  - <sup>41</sup>Yu. A. Batusov *et al.*, Yad. Fiz. 23, 1169 (1976) [Sov. J. Nucl. Phys. 23, 621 (1976)].
  - <sup>42</sup>E. Gadioli and Erba Gadioli, Nucl. Phys. A256, 414 (1976).
  - <sup>43</sup>D. A. Arsen'ev and G. G. Bunatyan, Preprint R4-8835 [in Russian], JINR, Dubna (1975).
  - <sup>44</sup>C. J. Orth *et al.*, Preprint LA-UR-78-2686, Los Alamos (1978).
  - <sup>45</sup>M. Leon and R. Seki, Nucl. Phys. A282, 445 (1977).
  - <sup>46</sup>M. Leon and J. H. Miller, Nucl. Phys. A282, 461 (1977).
  - <sup>47</sup>V. S. Barashenkov *et al.*, Usp. Fiz. Nauk 109, 91 (1973) [Sov. Phys. Usp. 16, 31 (1974)].
  - <sup>48</sup>M. Blann, Ann. Rev. Nucl. Sci. 25, 123 (1975).
  - <sup>49</sup>E. Gadioli, Erba Gadioli, and G. Tagliaferri, Riv. Nuovo Cimento 6, 1 (1976).
  - <sup>50</sup>K. K. Gudima, G. A. Ososkov, and V. D. Toneev, Yad. Fiz. 21, 260 (1975) [Sov. J. Nucl. Phys. 21, 138 (1975)].
  - <sup>51</sup>S. G. Mashnik and V. D. Toneev, Preprint R4-8417 [in Russian], JINR, Dubna (1974).
  - <sup>52</sup>V. Weisskopf, Phys. Rev. 52, 295 (1937).
  - <sup>53</sup>N. Bohr and J. A. Wheeler, Phys. Rev. 56, 426 (1939).
  - <sup>54</sup>I. Dostrovsky, Z. Fraenkel, and G. Friedlander, Phys. Rev. 116, 683 (1959).
  - <sup>55</sup>I. Dostrovsky, H. Gauvin, and M. Lefort, Phys. Rev. 169, 836 (1968).
  - <sup>56</sup>V. S. Barashenkov *et al.*, Nucl. Phys. A206, 131 (1973).
  - <sup>57</sup>R. Hartmann, Nucl. Phys. A308, 345 (1978).
  - <sup>58</sup>A. S. Il'inov *et al.*, Preprint P-0151 [in Russian], Institute of Nuclear Research, USSR Academy of Sciences, Moscow (1980).
  - <sup>59</sup>N. S. Muckhopadhyay, J. Hadernann, and K. Junker, Preprint PR-77-017, SIN (1977); Nucl. Phys. A319, 448 (1979).
  - <sup>60</sup>Yu. G. Budyashov *et al.*, Zh. Eksp. Teor. Fiz. 62, 21 (1972) [Sov. Phys. JETP 35, 13 (1972)].
  - <sup>61</sup>P. Casteleberry *et al.*, Phys. Lett. B34, 57 (1971).
  - <sup>62</sup>J. Comiso *et al.*, Phys. Rev. Lett. 35, 13 (1975).
  - <sup>63</sup>W. Dey *et al.*, Helv. Phys. Acta 49, 778 (1976).
  - <sup>64</sup>H. S. Pruijs *et al.*, in: Proc. Conf. on Nuclear Reaction Mechanisms, Varenna (1977).
  - <sup>65</sup>G. Mechttersheimer *et al.*, Phys. Lett. B73, 115 (1978).
  - <sup>66</sup>F. M. Schlepütz *et al.*, Phys. Rev. C 19, 135 (1979).
  - <sup>67</sup>A. S. Il'inov *et al.*, Kratk. Soobshch. Fiz. No. 11, 14 (1979).
  - <sup>68</sup>B. Bétak and P. Obložinsky, Contribution to the Intern. Symposium on Interactions of Fast Neutrons with Nuclei, Gauging (1975).
  - <sup>69</sup>S. Ozaki *et al.*, Phys. Rev. Lett. 4, 533 (1960).
  - <sup>70</sup>M. E. Nordberg, K. Kinsey, and R. L. Burman, Phys. Rev. 165, 1096 (1968).
  - <sup>71</sup>D. M. Lee *et al.*, Nucl. Phys. A197, 106 (1972).
  - <sup>72</sup>D. M. Lee *et al.*, Nucl. Phys. A182, 20 (1972).
  - <sup>73</sup>H. K. Walter *et al.*, Helv. Phys. Acta 50, 561 (1977).
  - <sup>74</sup>B. Bassalleck *et al.*, Phys. Lett. B65, 128 (1976).
  - <sup>75</sup>B. Bassalleck *et al.*, Phys. Rev. C 16, 1526 (1977).
  - <sup>76</sup>B. Bassalleck *et al.*, Z. Phys. A286, 401 (1978).
  - <sup>77</sup>H. S. Pruijs *et al.*, Preprint PR-78-007, SIN (1978); Nucl. Phys. A316, 365 (1979).
  - <sup>78</sup>H. Ullrich *et al.*, Phys. Rev. Lett. 33, 433 (1974).
  - <sup>79</sup>F. E. Bertrand and R. W. Peelle, Phys. Rev. C 8, 1045 (1973).
  - <sup>80</sup>S. R. Avramov *et al.*, in: Proc. Sixth Intern. Conf. on High Energy Physics and Nuclear Structure, Santa Fe (1975), p. 190.
  - <sup>81</sup>V. S. Butsev *et al.*, Pis'ma Zh. Eksp. Teor. Fiz. 21, 400 (1975); 24, 117 (1976) [JETP Lett. 21, 182 (1975); 24, 103 (1976)].
  - <sup>82</sup>V. M. Abazov *et al.*, Nucl. Phys. A274, 463 (1976).
  - <sup>83</sup>V. S. Butsev *et al.*, Nucl. Phys. A285, 379 (1977).
  - <sup>84</sup>V. S. Butsev, Preprint R15-10847 [in Russian], JINR, Dubna (1977).
  - <sup>85</sup>V. M. Abazov *et al.*, Yad. Fiz. 27, 886 (1978) [Sov. J. Nucl. Phys. 27, 471 (1978)].
  - <sup>86</sup>V. M. Abazov, V. S. Butsev, and G. L. Butseva, Preprint E15-11713, JINR, Dubna (1978).
  - <sup>87</sup>V. S. Butsev, Izv. Akad. Nauk SSSR, Ser. Fiz. 43, 131 (1979).
  - <sup>88</sup>R. Beetz *et al.*, Z. Phys. A286, 215 (1978).
  - <sup>89</sup>V. M. Abazov *et al.*, Preprint R13-8079 [in Russian], JINR, Dubna (1974).
  - <sup>90</sup>S. S. Gershtein, Usp. Fiz. Nauk 124, 455 (1978) [Sov. Phys. Usp. 21, 223 (1978)].
  - <sup>91</sup>Y. Cassagnou *et al.*, Phys. Rev. C 16, 741 (1977).
  - <sup>92</sup>C. E. Stronach *et al.*, Nucl. Phys. A308, 290 (1978).
  - <sup>93</sup>W. Seelmann *et al.*, Preprint, Institut für Radiochemie, Kernforschungszentrum, Karlsruhe (1975).
  - <sup>94</sup>J. R. Wu, C. C. Chang, and H. D. Holmgren, Phys. Rev. C 19, 698 (1979).
  - <sup>95</sup>H. A. Thiessen, in: Proc. Fifth Intern. Conf. on High Energy Physics and Nuclear Structure, Uppsala (1973), p. 416.

- <sup>96</sup>A. S. Il'inov, V. I. Nazaruk, and S. E. Chigrinov, Preprint P-0022 [in Russian], Institute of Nuclear Research, USSR Academy of Sciences, Moscow (1975); in *Tezisy dokladov XXVI soveshchaniya po yadernoi spektroskopii i strukture atomnogo yadra* (Proc. 26th Symposium on Nuclear Spectroscopy and Nuclear Structure), Leningrad (1976), p. 260.
- <sup>97</sup>M. P. Locher and F. Myhrer, *Helv. Phys. Acta* **49**, 123 (1976).
- <sup>98</sup>A. S. Il'inov and V. I. Nazaruk, in: *Tr. vsesoyuz. seminara po programme éksperimentov na mezonnoi fabrike* (Proc. All-Union Seminar on the Program of Experiments in the Meson Factory), Zvenigorod (1977).
- <sup>99</sup>W. J. Kossler *et al.*, *Phys. Rev.* **46**, 1551 (1971).
- <sup>100</sup>S. W. Lewis *et al.*, *Phys. Lett.* **B47**, 339 (1973).
- <sup>101</sup>C. E. Stronach *et al.*, *Phys. Rev. C* **15**, 984 (1977).
- <sup>102</sup>W. John and W. F. Fry, *Phys. Rev.* **91**, 1234 (1953).
- <sup>103</sup>N. A. Perfilov, O. V. Lozhkin, and V. P. Shamov, *Zh. Eksp. Teor. Fiz.* **28**, 655 (1955) [*JETP* **1**, 439 (1955)].
- <sup>104</sup>G. E. Belovitskiĭ *et al.*, *Zh. Eksp. Teor. Fiz.* **29**, 537 (1955) [*JETP* **2**, 493 (1956)].
- <sup>105</sup>N. A. Perfilov and N. S. Ivanova, *Zh. Eksp. Teor. Fiz.* **29**, 551 (1955) [*JETP* **2**, 433 (1956)].
- <sup>106</sup>Yu. A. Batusov *et al.*, Preprint R15-8917 [in Russian], JINR, Dubna (1975).
- <sup>107</sup>U. Moser *et al.*, to be published.
- <sup>108</sup>V. S. Butsev *et al.*, *Yad. Fiz.* **27**, 621 (1978) [*Sov. J. Nucl. Phys.* **27**, 332 (1978)].
- <sup>109</sup>E. Gadioli, Erba Gadioli, and A. Moroni, *Z. Phys.* **A288**, 39 (1978).
- <sup>110</sup>L. C. Moretto *et al.*, *Phys. Lett.* **B38**, 471 (1972).
- <sup>111</sup>A. V. Ignatyuk *et al.*, *Yad. Fiz.* **21**, 1185 (1975) [*Sov. J. Nucl. Phys.* **21**, 612 (1975)].
- <sup>112</sup>A. S. Il'inov, E. A. Cherepanov, and S. E. Chigrinov, *Z. Phys.* **A287**, 37 (1978).
- <sup>113</sup>J. R. Nix and E. Sassi, *Nucl. Phys.* **81**, 1 (1966).
- <sup>114</sup>V. S. Barashenkov and V. D. Toneev, *Vzaimodeistvie vyso-koénergeticheskikh chastits i atomnykh yader s yadrami* (Interaction of High Energy Particles and Nuclei with Nuclei), Moscow (1972).
- <sup>115</sup>W. D. Myers and W. J. Swiatecki, *Ark. Fyz.* **36**, 343 (1967); Preprint ISRL-11980, Berkeley (1965).
- <sup>116</sup>A. S. Il'inov and E. A. Cherepanov, Preprint P-0064 [in Russian], Institute of Nuclear Research, USSR Academy of Sciences, Moscow (1977).
- <sup>117</sup>N. T. Porile, B. J. Dropesky, and R. A. Williams, *Phys. Rev. C* **18**, 2231 (1978).
- <sup>118</sup>J. R. Nix, *Nucl. Phys.* **A130**, 241 (1969).
- <sup>119</sup>H. C. Pauli and T. Ledergerber, *Nucl. Phys.* **A175**, 545 (1971).
- <sup>120</sup>H. J. Krappe and J. R. Nix, in: *Proc. Third IAEA Symposium on the Physics and Chemistry of Fission*, Vol. 1 (1973), Paper IAEA-SM-174/12.
- <sup>121</sup>R. W. Hasse, *Ann. Phys. (Leipzig)* **68**, 377 (1971).
- <sup>122</sup>R. W. Hasse and W. Stocker, *Phys. Lett.* **B44**, 26 (1973).
- <sup>123</sup>G. Sauer, H. Chandra, and U. Mosel, *Nucl. Phys.* **A264**, 221 (1976).
- <sup>124</sup>M. Brack *et al.*, *Rev. Mod. Phys.* **44**, 320 (1972).
- <sup>125</sup>A. Gavron, H. C. Britt, and J. B. Wilhelmy, *Phys. Rev. C* **13**, 2577 (1976).
- <sup>126</sup>V. I. Kuznetsov, N. K. Skobelev, and G. N. Flerov, *Yad. Fiz.* **4**, 279 (1967); **5**, 271 (1967) [*Sov. J. Nucl. Phys.* **4**, 202 (1966); **5**, 191 (1966)]; N. K. Skobelev, *Yad. Fiz.* **15**, 444 (1972) [*Sov. J. Nucl. Phys.* **15**, 248 (1972)].
- <sup>127</sup>D. Z. Ganzorig *et al.*, Preprint E15-9365, JINR, Dubna (1975).
- <sup>128</sup>V. S. Butsev *et al.*, Preprint R15-12339 [in Russian], JINR, Dubna (1979).
- <sup>129</sup>D. Chultem *et al.*, *Nucl. Phys.* **A247**, 452 (1975).
- <sup>130</sup>B. Bassalleck *et al.*, *Nucl. Phys.* **A319**, 397 (1979).
- <sup>131</sup>A. B. Migdal, O. A. Markin, and I. N. Mishustin, *Zh. Eksp. Teor. Fiz.* **66**, 443 (1974); **70**, 1952 (1976) [*Sov. Phys. JETP* **39**, 212 (1974); **43**, 1015 (1976)].
- <sup>132</sup>A. B. Migdal, *Usp. Fiz. Nauk* **123**, 369 (1977) [*Sov. Phys. Usp.* **20**, 879 (1977)].
- <sup>133</sup>M. A. Troitskiĭ, M. V. Koldaev, and N. I. Chekunaev, *Zh. Eksp. Teor. Fiz.* **73**, 1258 (1977) [*Sov. Phys. JETP* **46**, 662 (1977)].
- <sup>134</sup>V. S. Butsev and D. Chultem, *Phys. Lett.* **B67**, 33 (1977).
- <sup>135</sup>A. K. Kerman and L. S. Kisslinger, *Phys. Rev.* **180**, 1483 (1969).
- <sup>136</sup>M. Goldhaber, in: *Proc. Intern. Conf. on Nuclear Physics*, Vol. 2, Munich (1973), p. 14.
- <sup>137</sup>B. Coupat *et al.*, *Phys. Lett.* **B55**, 286 (1975).
- <sup>138</sup>A. M. Green, *Rep. Prog. Phys.* **39**, 1109 (1976).
- <sup>139</sup>V. M. Abazov *et al.*, Preprint D6-11574 [in Russian], JINR, Dubna (1978), p. 58.
- <sup>140</sup>H. J. Pirner, *Phys. Lett.* **B69**, 170 (1977).
- <sup>141</sup>W. K. H. Panofsky, R. L. Aamodt, and J. Hadley, *Phys. Rev.* **81**, 565 (1951).
- <sup>142</sup>W. K. H. Panofsky, R. L. Aamodt, and J. Hadley, *Phys. Rev.* **81**, 565 (1951).
- <sup>143</sup>J. C. Sens *et al.*, *Nuovo Cimento* **7**, 536 (1958).
- <sup>144</sup>G. Backenstoss *et al.*, *Bull. Am. Phys. Soc.* **11**, 273 (1958).
- <sup>145</sup>A. Astbury *et al.*, *Nuovo Cimento* **18**, 1267 (1960).
- <sup>146</sup>J. E. Lathrop, *Nuovo Cimento* **15**, 831 (1960).
- <sup>147</sup>M. Eckhause *et al.*, *Nuovo Cimento* **24**, 666 (1962).
- <sup>148</sup>J. S. Baijal *et al.*, *Nuovo Cimento* **30**, 711 (1963).
- <sup>149</sup>L. I. Ponomarev and Yu. D. Prokoshkin, *Comments Nucl. Part. Phys.* **2**, 176 (1965).
- <sup>150</sup>V. G. Zinov, A. D. Konin, and A. I. Mukhin, *Yad. Fiz.* **2**, 859 (1965) [*Sov. J. Nucl. Phys.* **2**, 613 (1966)].
- <sup>151</sup>Yu. G. Budyashov *et al.*, *Yad. Fiz.* **5**, 591 (1966) [*Sov. J. Nucl. Phys.* **5**, 420 (1966)].
- <sup>152</sup>M. Y. Au-Yang and M. L. Cohen, *Phys. Rev.* **174**, 468 (1968).
- <sup>153</sup>L. I. Ponomarev, *Ann. Rev. Nucl. Sci.* **23**, 395 (1973).
- <sup>154</sup>P. W. Vogel *et al.*, *Nucl. Phys.* **A245**, 445 (1975).
- <sup>155</sup>V. D. Bobrov *et al.*, *Zh. Eksp. Teor. Fiz.* **48**, 1197 (1965) [*Sov. Phys. JETP* **21**, 798 (1965)].
- <sup>156</sup>J. D. Knight *et al.*, *Phys. Rev. A* **13**, 43 (1976).
- <sup>157</sup>L. Tauscher *et al.*, *Phys. Lett.* **A27**, 581 (1968).
- <sup>158</sup>G. A. Grin and R. Kunselman, *Phys. Lett.* **B31**, 116 (1970).
- <sup>159</sup>W. K. H. Panofsky, R. L. Aamodt, and J. Hadley, *Phys. Rev.* **8**, 565 (1951).
- <sup>160</sup>V. I. Petrukhin, Yu. D. Prokoshkin, and A. I. Filippov, *Yad. Fiz.* **6**, 1008 (1967) [*Sov. J. Nucl. Phys.* **6**, 734 (1967)].
- <sup>161</sup>S. S. Gershtein, *Usp. Fiz. Nauk* **97**, 3 (1969) [*Sov. Phys. Usp.* **12**, 1 (1969)].
- <sup>162</sup>H. Daniel, *Phys. Rev. Lett.* **35**, 1649 (1975).
- <sup>163</sup>V. I. Petrukhin and V. M. Surorov, *Zh. Eksp. Teor. Fiz.* **70**, 1145 (1976) [*Sov. Phys. JETP* **43**, 595 (1976)].
- <sup>164</sup>V. A. Vasil'ev *et al.*, Preprint R1-10222 [in Russian], JINR, Dubna (1976).
- <sup>165</sup>V. S. Butsev, Preprint E15-9658, JINR, Dubna (1976); *Phys. Lett.* **B63**, 47 (1976).
- <sup>166</sup>H. Daniel, *Nucl. Instrum. Methods* **150**, 609 (1978).
- <sup>167</sup>V. M. Abazov *et al.*, in: *Tr. mezhdunarodnogo simpoziuma po problemam mezonnoi khimii i mezomolekulyarnykh protsessov* (Proc. Intern. Symposium on Problems of Mesic Chemistry and Mesomolecular Processes), Dubna (1977), p. 127.
- <sup>168</sup>V. M. Abazov *et al.*, Preprint E15-12013, JINR, Dubna (1978).
- <sup>169</sup>Z. Lewandowski *et al.*, *Phys. Lett.* **B80**, 350 (1979).
- <sup>170</sup>R. Bizzarri *et al.*, *Nuovo Cimento* **33**, 1497 (1964).
- <sup>171</sup>M. M. Block *et al.*, *Phys. Rev. Lett.* **11**, 301 (1963).
- <sup>172</sup>O. A. Zaimidoriga, R. N. Sulyaev, and V. M. Tsupko-Sitnikov, *Zh. Eksp. Teor. Fiz.* **52**, 97 (1967) [*Sov. Phys. JETP* **25**, 63 (1967)].
- <sup>173</sup>C. E. Brown and W. Weise, *Phys. Rev. C* **27**, 1 (1976).

Translated by Julian B. Barbour